Dynamics of Predissociation in the Condensed Phase: Markovian Master Equation

Irene Burghardt[†]

Institut für Physikalische und Theoretische Chemie der Universität Bonn, Wegelerstrasse 12, 53115 Bonn, Germany

Received: November 14, 1997; In Final Form: January 27, 1998

The effect of an environment on ultrafast predissociation processes is modeled in terms of a Markovian, Lindblad-type master equation in the coordinate representation. The analysis focuses on the effects of vibrational and electronic dephasing on one hand and "indirect", environment-induced electronic transitions on the other hand. The latter not only exert a quenching effect on coherent curve-crossing dynamics, as shown for a system exhibiting periodic Landau−Zener-type crossings, but may largely determine the dynamics if the system features no intrinsic electronic coupling. This provides a simplified description, restricted to the Markovian limit, for purely environment-induced processes such as the predissociation of I_2 in its $B0_u^+$ state. Numerical integration of the coordinate-space master equation is performed by a split-propagator technique. The problem of defining absorbing boundaries is solved by introducing an emission process, localized around the grid boundary, to an auxiliary state that is otherwise not involved in the dynamics.

1. Introduction

A number of recent time-resolved experiments have addressed the study of ultrafast predissociation phenomena in a condensed-phase or cluster environment. Notably, a detailed investigation of the solvent-induced predissociation of I_2 in a rare-gas environment has been carried out by Zewail and co-workers.[1,2] Further studies on this system include earlier work by Scherer et al.,[3] as well as recent experiments by Apkarian and co-workers in cryogenic matrixes[4] and by Chergui and co-workers for a liquid environment.[5] The recent investigation, by Kiefer and co-workers,[6] of the predissociation of NaI in a rare-gas surrounding complements earlier gas-phase studies[7,8] of this prototype system. Typically, the results of these experiments feature a stepwise depletion of the initially populated electronic state, possibly with nonexponential decay behavior at high pressures. Ultrafast curve-crossing dynamics in a many-body environment has further been studied for systems such as ICN, whose early-time dynamics involves dissociation via several potential surfaces,[9] as well as in biochemical systems, in particular the photoisomerization of rhodopsin[10] and the primary electron-transfer step in photosynthesis.[11]

Theoretical accounts of curve-crossing dynamics in the presence of an environment essentially follow two types of approaches. The first refers to a description, mostly of (semi)-classical nature, of the combined molecule-plus-environment system, which may amount to a collision model or scattering calculation to describe a dilute-gas situation, or a molecular-dynamics simulation to capture a liquid-state environment. An example of the former is given by the recent analysis of the predissociation of NaI by Engel and co-workers,[12] while semiclassical many-body simulations involving several electronic surfaces have been proposed by Coker and co-workers,[13] Jungwirth and Gerber,[14] Martens and co-workers,[15] and Levine and Fleming and co-workers[16] to describe the dynamics of I_2. The reliability of such studies is limited, on one hand, by the accuracy of the many-body potential-energy surfaces which are generally of semiempirical type and, on the other hand, by the semiclassical character of the dynamics. Even if a semiclassical approximation yields very good results for the dynamics of heavy-atom systems such as I_2 on a single Born−Oppenheimer surface, it is more difficult to capture the quantum coherence that is characteristic of curve-crossing situations.

The second avenue is given by the "reduced dynamics" approach, involving a master equation[17,18] that represents an equation of motion for the subsystem of interest (e.g., the diatomic molecule) while incorporating the effects of the environment. In the simplest case, the master-equation treatment amounts to introducing phenomenological relaxation and dephasing constants, while the most complete treatment involves a "memory kernel" that fully takes into account the combined dynamics of the system and environment. Rate equations, which provide a connection to the phenomenological treatment, emerge from the master equation in the Markovian limit,[17−19] which implies that the environmental fluctuations occur on a time scale that is very rapid as compared with the "system" dynamics. Markovian master equations have recently been applied to curve-crossing situations by a number of authors.[20−25] These studies highlight the role of vibrational coherence in the short-time dynamics, which precludes a conventional treatment of the nonadiabatic dynamics in terms of the rate expressions well known from the theory of electron transfer.[26−30] The reduced-dynamics approach offers the advantage of an accurate quantum-mechanical treatment of the subsystem of interest. Its shortcomings lie in losing the details of system−environment correlations on short time scales, which are well captured by simulations of the overall system.

Most of the above-mentioned studies based on the master equation refer to discrete vibrational basis sets, which may be handled analytically in the case of harmonic potentials.[22] Such basis sets are not suitable for dissociative systems, where a coordinate-space representation or a phase-space representation in terms of Wigner functions[24,31] is more adequate. The latter approach has very recently been applied to a curve-crossing problem by Tanimura and Maruyama,[32] and relatedly, a classical-limit formulation was proposed by Basilevsky and Voronin.[25] The present work takes an approach based on the

[†] Present address: Theoretische Chemie, Physikalisch-Chemisches Institut, Im Neuenheimer Feld 253, 69120 Heidelberg, Germany.

S1089-5639(98)00220-5 CCC: $15.00
Published on Web 04/14/1998

coordinate-space representation, using a numerical short-time ("split-propagator") propagation scheme. This represents an alternative to the global coordinate-space propagators which have been applied in a number of works by Kosloff and co-workers.[33−37]

We investigate the predissociation dynamics of an electronic two-state system, using a Markovian master equation of semigroup type.[19,38−40] To motivate the form of certain elements of the master equation, we build a bridge to another formulation of the Markovian master equation, in terms of Redfield theory.[18,41−43] The physical effects we focus upon are "indirect", i.e., fluctuation-induced, transitions between the electronic states, as well as vibrational and electronic dephasing. The problem of defining "absorbing boundaries" to prevent reflection effects due to the finite extension of the coordinate-space grid is solved by introducing a "spontaneous emission" process localized in coordinate space, such that a complete damping of the density matrix elements takes place close to the grid boundary.

This model for the electronic two-state system allows us to study the competition between coherent and incoherent, i.e., fluctuation-induced, mechanisms of electronic coupling, as well as the role of dephasing. Several scenarios are studied, one of which corresponds to periodic Landau−Zener-type crossings similar to those observed for NaI,[6−8] while another represents an example of purely "incoherent" electronic coupling. The latter leads to environment-induced electronic transitions in the Markovian-limit dynamics and will be shown to provide a model approach to the solvent-induced predissociation of I_2. Notice here that the Markovian limit represents the most extreme case as far as destruction of coherent dynamics—characteristic of wavepacket dynamics in the isolated system—is concerned. A more realistic description, allowing for similar time scales of system and environment evolution, will tend to conserve coherence on a longer time scale. Such non-Markovian approaches have recently been pursued by Tanimura and Murayama[32] as well as Coalson and co-workers.[28] However, the Markovian treatment provides a convenient description in terms of energy relaxation ("T_1 -type" process) and phase, or coherence, relaxation ("T_2 -type" process). Such classification gives a useful guideline for the description of the dynamics, even though a non-Markovian treatment may eventually be required.

The plan of the paper is as follows. Section 2 gives a short description of the system and specifies the interaction with the environment. Section 3 introduces the Markovian master equation used in this work. In section 4, we point out the relevance, in the context of the reduced dynamics treatment, of the complex eigenvalues of the Liouvillian. Here, we also discuss the relation of our results to the spectroscopic signal, in the impulsive limit. Section 5 gives a description of the numerical method, and section 6 proposes results for several model situations. The last section gives a short discussion and conclusion.

2. System Hamiltonian and System−Bath Interaction

We consider a predissociation process for a diatomic molecule embedded in an environment. For simplicity, we restrict the treatment to two electronic states, one of which is dissociative. The Hamiltonian for the isolated molecule may be represented as a matrix in the basis of electronic states $\{|n^S\rangle\}$,

$$\hat{H}_S = \sum_{n,m=1,2} [\hat{T}^S_{nm} + \hat{V}^S_{nm}(\mathbf{r}_S)]|n^S\rangle\langle m^S| \qquad (1)$$

where the kinetic and potential operators on the rhs act only on the nuclear wave functions. The system−environment interaction, in the same basis, takes the general form

$$\hat{H}_{SB} = \sum_{n,m=1,2} \hat{h}^{SB}_{nm}(\mathbf{r}_S, \mathbf{r}_B)|n^S\rangle\langle m^S| \qquad (2)$$

where $\{\mathbf{r}_S, \mathbf{r}_B\}$ collectively denote the nuclear coordinates of the molecule and the environment, respectively. (In the present context, we do not need to consider explicitly the electronic degrees of freedom for the environment species, which are assumed to remain in their electronic ground state $|n^B_0\rangle$. In principle, the interaction Hamiltonian should be formulated for an antisymmetrized direct-product basis of electronic states $\mathcal{A}\{|n^S\rangle\langle m^S|\otimes|n^B_0\rangle\langle n^B_0|\}$, where $\mathcal{A}$ is the antisymmetrizer which guarantees that the electrons of the combined molecule-plus-environment system obey fermion exchange symmetry.) We will choose as the "system" coordinate r_S the internuclear distance in the diatomic molecule, while $\mathbf{r}_B$ denotes all relative coordinates between the diatomic and the environment species. The electronic basis states $\{|n^S\rangle\}$ may be chosen to correspond to the diabatic or adiabatic representation (see below). The kinetic-energy operator $\hat{T}^S$ refers to the nuclear kinetic energy throughout and may have off-diagonal elements depending on the chosen representation.

The numerical calculations presented in this paper are carried out in the diabatic representation for the two-state Hamiltonian of the diatomic molecule, with $\hat{T}^S$ being diagonal in the electronic states, $\hat{T}^S_{nm} = -\hbar^2\Delta_r/(2\mu)\,\delta_{nm}$ with the reduced mass μ and the Laplacian Δ_r, while off-diagonal potential couplings, $\hat{V}^S_{nm}(r_S)$, may occur. These diabatic coupling matrix elements may be due to spin−orbit interaction or other system-intrinsic couplings, or possibly to an average coupling due to the environment, within a "reduced dynamics" description.[17] (Notice that the diabatic basis is defined here in a loose sense; for a discussion of this issue, see, for example, refs 44 and 46.) On diagonalization of the potential-energy part, the Born−Oppenheimer or adiabatic potential-energy surfaces are obtained, with $\hat{V}^S_{nm}(r_S) = \hat{V}^S_{nm}(r_S)\,\delta_{nm}$. These may feature, in particular, avoided crossings due to the off-diagonal matrix elements of the diabatic representation. In the adiabatic representation, off-diagonal terms occur in the kinetic-energy part, which involve first and second derivatives in the nuclear coordinates. For an electronic two-level system and a single nuclear coordinate r_S, the two representations are related by the unitary transformation

$$\mathbf{U}(r_S) = \begin{pmatrix} \cos\theta(r_S)/2 & \sin\theta(r_S)/2 \\ -\sin\theta(r_S)/2 & \cos\theta(r_S)/2 \end{pmatrix} \qquad (3)$$

where $\tan\theta(r_S) = -2V_{12}(r_S)/[V_{11}(r_S) - V_{22}(r_S)]$, with the matrix elements defined with respect to the diabatic representation. The parameter θ may be chosen in the range $[0, \pi]$ such that the labeling of the diabatic and corresponding adiabatic states coincides asymptotically. Starting from the calculation in the diabatic representation, we may derive the corresponding quantities in the adiabatic representation using the above transformation. Notice that the diabatic representation is often more convenient for numerical implementation since the derivative couplings pertaining to the adiabatic representation are in general rapidly varying functions of the nuclear coordinates.[44] For a similar reason, certain observable quantities may be related to the diabatic rather than the adiabatic representation, as pointed out by Domcke and co-workers.[44,45]

The interaction with the environment comprises, in the general case, diagonal and off-diagonal matrix elements $\hat{h}^{SB}_{nm}(r_S, \mathbf{r}_B)$.

Fluctuations in an off-diagonal coupling element $\hat{h}^{SB}_{nm}$, $n \neq m$, in the diabatic representation translate into fluctuations of the energy gap ($\Delta = 2|V_{12}(r_X)|$ at the crossing point r_X, for the isolated molecule) in the adiabatic representation. The role of the off-diagonal elements will be most conspicuous in cases where the interaction with the environment breaks the symmetry of the unperturbed system. For example, in a diatomic molecule, two states of different parity are allowed to cross in the isolated molecule, while the symmetry-breaking due to the environment generates off-diagonal coupling elements. In this particular case, where the system features no intrinsic coupling that may induce curve-crossing dynamics, such environment-induced couplings can have a dominant effect on the time evolution. In this context, the solvent-induced predissociation of I_2 provides an example that has been extensively discussed in the recent literature.[1−5] The role of such off-diagonal couplings has further been considered in physical situations such as collisions between atomic species[47,48] and interactions between atoms and surfaces.[49] In the present analysis, we will consider cases where such couplings give rise to "relaxation-like" effects, that is, in the limit of rapid environmental fluctuations that induce transitions between the electronic states of the diatomic molecule. Such effects are closely related to the effects of spontaneous emission that have recently been discussed in the context of curve-crossing situations in quantum optics.[50−52]

3. Reduced Dynamics: Semigroup Treatment

3.1. General Considerations. The subsystem dynamics, given by equations of motion for the reduced "system" density operator $\hat{\rho}_S = \mathrm{Tr}_B\, \hat{\rho}$, with the degrees of freedom of the environment integrated out by the trace (Tr_B) operation, is rigorously given in terms of the generalized master equation.[17,53] While application of the latter may present a rather difficult task, a number of simplified treatments exist that are based, in particular, on the following assumptions: (i) A separation of time scales exists for the "system" and "environment" evolution (Markovian approximation), as implied by the condition $\lambda\tau_c \ll 1$, where λ denotes the coupling strength associated with the interaction Hamiltonian $\hat{H}_{SB}$, and τ_c is the correlation time for the fluctuations in the environmental dynamics:[17−19] Rapid environmental fluctuations induce transitions in the "system" whose intrinsic dynamics is much slower. (ii) The system−bath interaction Hamiltonian, with its general form as given in eq 2, factorizes in terms of "system" and "bath" operators $\hat{s}_{nm}(\mathbf{r}_S)$ and $\hat{b}_{nm}(\mathbf{r}_B)$ acting on the respective nuclear degrees of freedom: $\hat{H}_{SB} = \sum_{n,m} \hat{s}_{nm}(\mathbf{r}_S)\, \hat{b}_{nm}(\mathbf{r}_B)|n^S\rangle\langle m^S|$. Frequently, a coupling bilinear in the system and bath coordinates (like in the path integral approach[54]) or a quadratic form in the system coordinate[22,24] is assumed.

While the Markovian approximation is questionable for systems that exhibit rapid "system" evolution in the presence of an environment evolving on a similar time scale—i.e., the typical case in ultrafast molecular dynamics—it is nevertheless frequently applied, in view of the complexity of the non-Markovian treatment. Two principal formulations of the Markovian dynamics are currently being used: (i) the Redfield equations,[41] which are obtained by keeping terms up to second order in the cumulant expansion of the generalized master equation;[18] (ii) semigroup methods,[38−40] which bear a close analogy to Redfield theory, but are explicitly constructed such as to meet a positivity requirement on the reduced density operator. The semigroup property implies that the time evolution can be determined from a differential equation $(\mathrm{d}/\mathrm{d}t)\hat{\rho}_S = \mathcal{L}_{\mathrm{reduced}}\hat{\rho}_S$, which has to preserve the properties of the density operator, i.e., trace conservation and positivity. (In fact, the positivity requirement is not necessarily met by a master equation in the Markovian limit. For a discussion of the physical origin of the violation of positivity, see the recent discussion in refs 55 and 56.) The Redfield approach is generally applied in the vibrational or vibronic eigenstate representation[42,43] and yields transition rates related to the spectral density provided by the environmental fluctuations. The semigroup treatment rather takes a semiphenomenological view by introducing rate constants for different relaxation or dephasing-type processes. The latter has been applied, in particular, to density matrix propagation in the coordinate representation.[33−37]

Markovian reduced dynamics offers a convenient classification of different processes and phenomena: in particular, dephasing and energy relaxation processes are naturally distinguished. This neat distinction may not carry over to the non-Markovian case. The inherent disadvantage of the Markovian approach, basically due to the assumption of the separation of "system" and "bath" time scales, is that the details of system−bath correlations are essentially lost. Such correlations may be especially important if the system evolves rapidly.

In the present work, we apply semigroup methods to the study of predissociation processes of diatomic molecules embedded in an environment. A representation of the density operator in coordinate space is used, which is particularly suitable for the treatment of dissociative dynamics. We center on the early-time events in the excited-state dynamics and disregard the dynamics due to the deformation of the solute potential by the solvent, along with recombination effects. In the curve-crossing dynamics, we distinguish the effects of "direct" (or coherent) couplings and "indirect" (or incoherent) couplings due to the environment and analyze their interference. In the simplest case, successive Landau−Zener-type transitions, as encountered, for example, in NaI,[6−8] are found to be damped by the effects of the indirect coupling. This effect bears a close analogy with the effect of spontaneous emission on Landau−Zener transitions, which has been recently investigated.[50−52] Another scenario relates to the indirect coupling inducing transitions between electronic states in the absence of a direct coupling. We further point to the role of vibrational and electronic coherence, which can be associated with the spectrum of complex eigenvalues of the Liouvillian that characterize the dynamics of the system.

3.2. Markovian Master Equation. The master equation separates the temporal evolution of the reduced density operator, $\hat{\rho}_S = \mathrm{Tr}_B\, \hat{\rho}$, into a coherent and a dissipative part,

$$\frac{\mathrm{d}}{\mathrm{d}t}\hat{\rho}_S = \mathcal{L}_S\hat{\rho}_S + \mathcal{L}_{\mathrm{diss}}\hat{\rho}_S \tag{4}$$

with the coherent part involving the Hamiltonian $\hat{H}_S$ of eq 1, which may include an average system−bath coupling, $\langle\hat{H}_{SB}\rangle$,[17]

$$\mathcal{L}_S\hat{\rho}_S = -\frac{\mathrm{i}}{\hbar}[\hat{H}_S, \hat{\rho}_S] \tag{5}$$

and the dissipative part chosen to correspond to the Lindblad form,[38,39]

$$\mathcal{L}_{\mathrm{diss}}\hat{\rho}_S = \frac{1}{\hbar^2}\sum_i \left\{\hat{C}_i\hat{\rho}_S\hat{C}_i^\dagger - \frac{1}{2}(\hat{C}_i^\dagger\hat{C}_i\hat{\rho}_S + \hat{\rho}_S\hat{C}_i^\dagger\hat{C}_i)\right\} \tag{6}$$

where the $\hat{C}_i$ may be Hermitian or non-Hermitian (typically, level-shift) operators acting on the electronic and/or nuclear degrees of freedom of the system.[39,40] Notice that the symbol $\mathcal{L}$ henceforth refers to the Liouvillian superoperator as well as its representation in a particular basis. In the present context,

L_{diss} comprises the following operators:

$$\hat{C}_{12,\text{el}} = |1\rangle\langle 2|\sqrt{\Gamma_{12}(\hat{r})}; \quad \hat{C}_{21,\text{el}} = |2\rangle\langle 1|\sqrt{\Gamma_{21}(\hat{r})}$$

$$\hat{C}_{11,\text{el}} = |1\rangle\langle 1|\sqrt{\Gamma_{11,\text{el}}}; \quad \hat{C}_{22,\text{el}} = |2\rangle\langle 2|\sqrt{\Gamma_{22,\text{el}}}$$

$$\hat{C}_{11,\text{vib}} = |1\rangle\langle 1|\sqrt{\Gamma_{11,\text{vib}}}(\hat{r} - r_1^0); \qquad \hat{C}_{22,\text{vib}} = |2\rangle\langle 2|\sqrt{\Gamma_{22,vib}}(\hat{r} - r_2^0)$$

$$\hat{C}_{X2,\text{el}} = |X\rangle\langle 2|\sqrt{\Gamma_{X2}(\hat{r})} \tag{7}$$

The rates Γ_i may be functions of the "system" nuclear coordinate operator $\hat{r} = \hat{r}_S$, in the same fashion as a potential operator; for clarity, the coordinate argument is explicitly indicated as an operator. The dephasing rates $\Gamma_{nn,\text{el}}$ and $\Gamma_{nn,\text{vib}}$ are chosen to be coordinate-independent, but the operators associated with the latter are linear in the coordinate operator $\hat{r}$. The operators $\hat{C}_{12,\text{el}}$ and $\hat{C}_{21,\text{el}}$ interconnect the electronic states 1 and 2. $\hat{C}_{X2,\text{el}}$ refers to a numerical device that involves a "spontaneous emission" process from the dissociative state $|2\rangle$ to an auxiliary state $|X\rangle$. This device serves to implement "absorbing boundaries" in the predissociation scenario under study. In the following, the physical processes associated with the above operators will be discussed in some detail.

1. "Indirect" Electronic Transition Processes Mediated by the Environment, Associated with $\hat{C}_{nm,\text{el}}$, $n \neq m$. Such processes stem from the presence of off-diagonal coupling terms, $\hat{h}_{nm}^{\text{SB}}$ with $n \neq m$, in the system−bath interaction Hamiltonian of eq 2. In the present context, the transitions are assumed to be driven by thermal fluctuations in the environment. Hence we should expect such transitions to take place predominantly in the vicinity of the (avoided) crossing. We assume here a Lorentzian dependence of the transition rate on the coordinate-dependent energy gap, $\Gamma_{\text{el}}(r) = \Gamma_0/([\Delta V_{12}(r)/\lambda]^2 + 1)$, where $\Delta V_{12}(r) = (V_{11}(r) - V_{22}(r))$, and λ is a parameter that defines the width of the distribution (which may be associated with the spectral density of the environment). The larger of the "up" and "down" rates, $\Gamma_{12}(r)$ and $\Gamma_{21}(r)$, is identified with $\Gamma_{\text{el}}(r)$, while the other is adjusted according to the detailed-balance condition

$$\frac{\Gamma_{12}(r)}{\Gamma_{21}(r)} = \exp\left(-\frac{\Delta V_{12}(r)}{kT}\right) \tag{8}$$

This type of coordinate-dependent rates associated with Lindblad operators involving electronic transitions have been recently applied by Saalfrank and Kosloff[36] in the context of photoinduced desorption processes on surfaces. The Appendix gives an alternative approach to the problem, based on the Redfield equations.[41,18] The latter approach offers some physical understanding of the coordinate dependence of the relaxation operators, based on a simple model for the system−bath interaction. A master equation is obtained that is similar but not identical to the Lindblad form of eq 6 with $\hat{C}_{12,\text{el}}$ and $\hat{C}_{21,\text{el}}$.

2. Electronic "Pure Dephasing", Associated with $\hat{C}_{nn,el}$. This process is related not to transitions between the electronic states but to fluctuations in the energy of the individual electronic states, which induce dephasing of electronic coherence. Notice that the overall electronic dephasing effect is composed of contributions due to both electronic transitions and "pure dephasing" (by analogy with the relation between T_1 and T_2 for a two-level system, $1/T_2 = 1/(2T_1) + 1/T_2^{\star}$, where $T_2^{\star}$ is the pure-dephasing constant).

3. Vibrational Dephasing, Associated with $\hat{C}_{nn,vib}$. Since vibrational dephasing, rather than vibrational energy relaxation, often provides the dominant effect in short-time dynamics,[57] we restrict the analysis to the dephasing effect. In the master equation, the operator $\hat{C}_{nn,\text{vib}}$ leads to the term $-\Gamma_{nn,\text{vib}}(r - r')^2 \rho_{nn}(r, r')$ for a given electronic state, which may be denoted "fluctuation" or "diffusion" term.[58−61] In the absence of the associated friction terms,[58−61] no energy relaxation takes place, but the system approaches an infinite-temperature limit. (As pointed out in ref 59, the dephasing term considered here yields the simplest type of master equation for an oscillator that is compatible with the Lindblad form, without, however, taking into account energy dissipation.) In the present model, this does not pose a problem, since the other mechanisms—"indirect" transitions and loss of density due to predissociation—lead to an overall loss of energy, possibly apart from a very short transient phase.

Let us comment shortly on the form of the dephasing term. It can be derived from the part of the system−bath Hamiltonian diagonal in the electronic states, with a coupling bilinear in the "system" and "bath" coordinates, $\hat{h}_{nm}^{\text{SB}}(r_S, \mathbf{r}_B) = \sum_i \xi_i(\hat{r}_S - r_S^0) \times (\hat{r}_B^i - r_B^{i,0})$. This coupling is of the conventional form and can be interpreted in terms of a Taylor expansion about the equilibrium positions r_S^0 and $r_B^{i,0}$ for coupled oscillators. The parameters r_n^0 associated with $\hat{C}_{nn,\text{vib}}$ then correspond to r_S^0 for a given electronic state. The dephasing gives rise to the decay of the coordinate-space coherences $\rho_{nn}(r, r')$, $r \neq r'$, with a quadratic dependence on the distance $|r - r'|$. This implies that "decoherence" first sets in at large distances. For wavepacket motion, for example, one should estimate the effect of the dephasing term on a scale $|r - r'|$ pertaining to the width of the wavepacket. Notice that the vibrational dephasing operator, as defined here, also affects the electronic coherence $\rho_{nm}(r, r')$, $n \neq m$ (see below).

4. "Spontaneous Emission" to a Third, Auxiliary State $|X\rangle$, Associated with $\hat{C}_{Xn,\text{el}}$. This represents a numerical device to implement "absorbing boundaries" for the dissociative electronic state involved in the predissociation process. Since we simulate the dynamics on a finite coordinate-space grid, reflection and wrap-around effects at the grid boundary introduce artifacts.[62] The problem is solved here as follows: An emission process, localized around the grid boundary with a suitable envelope function, takes place from the dissociative electronic state $|2\rangle$ to a third state $|X\rangle$. The form of the Lindblad operator $\hat{C}_{X2,\text{el}}$ guarantees that both the population of the dissociative state *and* electronic coherences between the nonadiabatically coupled states are damped efficiently (cf. the matrix representation of the Liouvillian given below). The method effectively simulates the dissociative ("Hilbert-space") continuum in terms of a dissipative ("Liouville-space") continuum localized in coordinate space. The numerical implementation is discussed further in section 5.

3.3. Matrix Representation of the Liouvillian: The Roles of "Direct" and "Indirect" Coupling. The present section provides a short discussion on the effects of "direct", or coherent, coupling intrinsic to the system, and "indirect", or environment-induced coupling arising from the dissipative part of the Liouvillian. Since the matrix representation of the Liouvillian is best suited to distinguish these effects, we give here the representation in the basis of (diabatic) electronic coherences and populations, $\{|1\rangle\langle 1|,$

$|2\rangle\langle 2|$, $|X\rangle\langle X|$, $|1\rangle\langle 2|$, $|2\rangle\langle 1|\}$. The population of the auxiliary state $|X\rangle$ is included since it allows one to consider the effect of the operator $\hat{C}_{X2}$; notice that no electronic coherences arise involving this state. The coherent and dissipative parts of the Liouvillian thus take the following matrix form:

$$L_S(r,r') = -\frac{i}{\hbar} \times$$

$$\begin{pmatrix}
\begin{matrix}-\hbar^2/(2\mu)(\Delta_r - \Delta_{r'})\\ +(V_{11}(r) - V_{11}(r'))\end{matrix} & 0 & 0 & -V_{21}(r') & V_{12}(r) \\
0 & \begin{matrix}-\hbar^2/(2\mu)(\Delta_r - \Delta_{r'})\\ +(V_{22}(r) - V_{22}(r'))\end{matrix} & 0 & V_{21}(r) & -V_{12}(r') \\
0 & 0 & 0 & 0 & 0 \\
-V_{12}(r') & V_{12}(r) & 0 & \begin{matrix}-\hbar^2/(2\mu)(\Delta_r - \Delta_{r'})\\ +(V_{11}(r) - V_{22}(r'))\end{matrix} & 0 \\
V_{21}(r) & -V_{21}(r') & 0 & 0 & \begin{matrix}-\hbar^2/(2\mu)(\Delta_r - \Delta_{r'})\\ +(V_{22}(r) - V_{11}(r'))\end{matrix}
\end{pmatrix} \tag{9}$$

$$L_{diss}(r,r') = \frac{1}{\hbar^2} \times$$

$$\begin{pmatrix}
\begin{matrix}-\frac{1}{2}\{\Gamma_{21}(r) + \Gamma_{21}(r')\\ +\Gamma_{11,vib}(r - r')^2\}\end{matrix} & \sqrt{\Gamma_{12}(r)}\sqrt{\Gamma_{12}(r')} & 0 & 0 & 0 \\
\sqrt{\Gamma_{21}(r)}\sqrt{\Gamma_{21}(r')} & \begin{matrix}-\frac{1}{2}\{\Gamma_{12}(r) + \Gamma_{12}(r')\\ +\Gamma_{22,vib}(r - r')^2\\ +\Gamma_{X2}(r) + \Gamma_{X2}(r')\}\end{matrix} & 0 & 0 & 0 \\
0 & \sqrt{\Gamma_{X2}(r)}\sqrt{\Gamma_{X2}(r')} & 0 & 0 & 0 \\
0 & 0 & 0 & \begin{matrix}-\frac{1}{2}\{\Gamma_{21}(r) + \Gamma_{12}(r')\\ +\Gamma_{X2}(r')\\ +\Gamma_{11,el} + \Gamma_{22,el}\\ +\Gamma_{11,vib}(r - r_1^0)^2\\ +\Gamma_{22,vib}(r' - r_2^0)^2\}\end{matrix} & 0 \\
0 & 0 & 0 & 0 & \begin{matrix}-\frac{1}{2}\{\Gamma_{21}(r') + \Gamma_{12}(r)\\ +\Gamma_{X2}(r)\\ +\Gamma_{11,el} + \Gamma_{22,el}\\ +\Gamma_{11,vib}(r' - r_1^0)^2\\ +\Gamma_{22,vib}(r - r_2^0)^2\}\end{matrix}
\end{pmatrix} \tag{10}$$

From the form of the Liouvillian L_S, it is evident that the coupling elements $V_{12} = V_{21}$ connect populations with coherences, such that population transfer occurs as a second-order process. In a semiclassical approximation, this leads to the Landau−Zener formula[63,64] for the transition probability between the two electronic states, $P_{12}^{LZ} = \exp[-2\pi V_{12}^2/(\hbar v|F_2 - F_1|)]$, where v denotes the velocity of the classical particle (or average velocity of the wavepacket), and $F_i = (dV_i/dr)$ are the slopes of the diabatic potential curves at the crossing.

Conversely, the "indirect" coupling causes direct transfer between the populations. Further, it acts as a quenching mechanism on the electronic coherences, which may be enhanced by the presence of "pure dephasing" due to $\Gamma_{nn,el}$ as well as $\Gamma_{nn,vib}$. Notice that the "spontaneous emission" process associated with the operator $\hat{C}_{X2}$ also acts on the electronic coherence.

The above form of L_{diss} is equally valid for the *adiabatic* electronic basis. In fact, if the system under investigation is of adiabatic rather than diabatic character (i.e., involving a large coupling constant V_{12}), it may be more adequate to choose the adiabatic basis for the dissipative part of the Liouvillian. Within the short-time propagation scheme, a switch of basis between the coherent and dissipative evolution steps is easily accommodated (see section 5). A substantial difference for the dissipative evolution arises, in particular, if electronic dephasing is considered: Since the transformation eq 3 converts adiabatic populations into a linear combination of diabatic populations *and* coherences, the latter will be strongly affected by a large dephasing rate $\Gamma_{nn,el}$, which translates back into a decay of the adiabatic populations.

4. Liouvillian Spectra and Observable Quantities

4.1. Coherent and Decay Dynamics: Complex Eigenvalues of the Liouvillian. Fundamentally, the time scales characterizing the coherent and decay dynamics of the system can be captured in terms of its resonances, i.e., metastable states with finite lifetimes. For example, for an isolated molecule undergoing predissociation, we may identify quasi-bound states

coupled to a dissociation continuum. Such resonance states are associated with complex energies $E_n = E_n^{\mathrm{r}} - \mathrm{i}\Gamma_n/2$ that may be identified by a number of different methods such as projection operator techniques,[66] complex scaling,[67] and other numerical techniques.[68]

In contrast to the above expression for the resonances in the Hilbert-space description, the complex eigenvalues in the Liouville-space description correspond to frequencies $\omega_{nm} = \omega_{nm}^{\mathrm{r}} - i\gamma_{nm}$. If we transpose the results for the isolated molecule to the Liouville-space description, we have $\omega_{nm}^{\mathrm{r}} = (E_n^{\mathrm{r}} - E_m^{\mathrm{r}})$ and $\gamma_{nm} = (\Gamma_n + \Gamma_m)/2$. If the interaction with an environment is added, further decay processes arise, which cannot be accommodated in a Hilbert-space description. Within the reduced-dynamics description, i.e., for a Liouvillian $L = L_{\mathrm{S}} + L_{\mathrm{diss}}$, we may consider the basis of eigenstates of L_{S},

$$L_{\mathrm{S}}|\phi_n\phi_m\rangle\rangle = -\frac{\mathrm{i}}{\hbar}\left[\omega_{nm}^{\mathrm{r}} - \frac{\mathrm{i}}{2}(\Gamma_n + \Gamma_m)\right]|\phi_n\phi_m\rangle\rangle \quad (11)$$

with the Liouville-space kets[31] $|\phi_n\phi_m\rangle\rangle = |\phi_n\rangle\langle\phi_m|$, given the eigenstates $|\phi_n\rangle$ of the Hamiltonian $\hat{H}_{\mathrm{S}}$. Notice that a basis of generalized eigenstates[69,70] is required for a non-Hermitian Hamiltonian or Liouvillian; however, in the present discussion, we do not explicitly indicate the distinction between left and right eigenvectors. Using the representation in terms of the Liouville-space basis defined above, the following expression for the Liouvillian including dissipation is obtained:

$$L = \sum_{n,m}|\phi_n\phi_m\rangle\rangle\left\{-\frac{\mathrm{i}}{\hbar}\left[\omega_{nm}^{\mathrm{r}} - \frac{\mathrm{i}}{2}(\Gamma_n + \Gamma_m)\right]\right\}\langle\langle\phi_n\phi_m| + \sum_{nm}\sum_{kl}|\phi_n\phi_m\rangle\rangle\{L_{\mathrm{diss}}\}_{nm,kl}\langle\langle\phi_k\phi_l| \quad (12)$$

Diagonalization of the overall Liouvillian yields a new basis $|\chi_j\rangle\rangle$ with eigenvalues $-i/\hbar(\omega_j^{\mathrm{r}} - i\gamma_j)$. Hence, we obtain for the propagator $U(t,t_0) = \exp[L\,(t - t_0)]$,

$$U(t, t_0) = \theta(t, t_0)\sum_j|\chi_j\rangle\rangle\exp\left\{-\frac{\mathrm{i}}{\hbar}[\omega_j^{\mathrm{r}} - \mathrm{i}\gamma_j](t - t_0)\right\}\langle\langle\chi_j| \quad (13)$$

where $\theta(t, t_0)$ is the Heaviside function imposing forward-time propagation.

If we consider the time evolution of the system, starting from an initial density operator $\hat{\rho}(t_0)$, we may infer the spectrum of complex eigenvalues of the Liouvillian from the correlation function

$$C(t, t_0) = \mathrm{Tr}\{\hat{\rho}^{\dagger}(t_0)\,\hat{\rho}(t)\} = \mathrm{Tr}\{\hat{\rho}(t_0)\,\hat{\rho}(t)\} = \sum_j\rho_j^{\dagger}(t_0)\,\rho_j(t_0)\exp\left\{-\frac{\mathrm{i}}{\hbar}[\omega_j^{r} - \mathrm{i}\gamma_j](t - t_0)\right\} \quad (14)$$

This correlation function is real and nonnegative, as can be seen for pure states by noting that $C(t, t_0) = |\langle\psi(t_0)\,\psi(t)\rangle|^2$. The extension to mixed states $\hat{\rho} = \sum_n p_n|\psi_n\rangle\langle\psi_n|$ yields, in a similar fashion, $C(t, t_0) = \sum_{n,m}p_n p_m|\langle\psi_n(t_0)\,\psi_m(t)\rangle|^2$. In section 6, we will discuss numerical examples of Fourier transforms of $C(t, t_0)$ yielding spectra that can be associated with the complex eigenvalues of the Liouvillian. The spectra are structured if discrete vibrational or vibronic transition frequencies are involved and feature a broadening due to the decay rates γ_j. In principle, one may numerically extract the underlying resonances from such spectra. We should generally expect that the dissipative rates affect not only the decay but also the real parts of the complex eigenfrequencies (see, for example, ref 40, where examples referring to few-level systems are discussed).

In the context of the numerical analysis, we will split up the above expression in terms of correlation functions for the individual electronic populations or coherences, $C(t, t_0) = \sum_{n,m}C_{nm}(t, t_0)$, with

$$C_{nm}(t, t_0) = \mathrm{Tr}_r\{\hat{\rho}_{mn}(t_0)\,\hat{\rho}_{nm}(t)\} = \int\mathrm{d}r\,\mathrm{d}r'\rho_{mn}(r, r'; t_0)\,\rho_{nm}(r', r; t) \quad (15)$$

where the $\hat{\rho}_{nm}$ are operators only with respect to the nuclear coordinates. This procedure may be useful to distinguish between vibrational and electronic (or vibronic) coherence, which may be associated with rather different frequencies ω_j in particular cases. For example, in curve-crossing systems that are of strongly adiabatic character, i.e., with a relatively large energy gap between the adiabatic electronic states, it may be feasible to distinguish between the vibrational coherence pertaining to a given electronic state and the vibronic coherence that is the signature of the coupling between the electronic states (see section 6.2.).

4.2. Observables and Quantities Characterizing the Dynamics. This paper focuses on a description of the excited-state dynamics, that is, on the time evolution of the density operator on the two electronic surfaces involved in the curve-crossing scenario. We monitor the correlation functions of eq 15 as well as the electronic populations and coherences in the diabatic and adiabatic representations. The relevant quantities are the norm for a given electronic state $\mathrm{Tr}_r\{\hat{\rho}_{nn}(t)\} = \int\mathrm{d}r\,\rho_{nn}(r, r; t)$, i.e., the integral over coordinate-space populations, as well as the quantities

$$|\rho_{nm}|(t) = [\mathrm{Tr}_r\{\hat{\rho}_{mn}(t)\,\hat{\rho}_{nm}(t)\}]^{1/2} \quad (16)$$

with $\mathrm{Tr}_{\mathrm{r}}\{\hat{\rho}_{mn}(t)\,\hat{\rho}_{nm}(t)\} = \int\mathrm{d}r\,\mathrm{d}r'\,\rho_{mn}(r, r'; t)\,\rho_{nm}(r', r; t)$. The two expressions are equal only for a pure state. Further, one may consider the expectation values of the coordinates and momenta for the individual electronic states, $\mathrm{Tr}_{\mathrm{r}}\{\hat{x}\hat{\rho}_{nn}\}$ and $\mathrm{Tr}_{\mathrm{r}}\{\hat{p}\hat{\rho}_{nn}\}$, which leads to a phase-space picture of the dynamics.

Since the numerical simulations presented here do not account for the excitation and detection process pertaining to a pump−probe-type experiment, the conclusions we may draw on the spectroscopic signal are limited. However, the excited-state density operator is of direct relevance to the signal in the impulsive limit, i.e., assuming that the laser pulses have an extremely short duration on the time scale of evolution under the molecular Hamiltonian. Recent work by Domcke and Stock[44,45] in the context of curve-crossing dynamics has shown that the results pertaining to the impulsive limit are generally in good agreement with exact calculations. Hence, the following subsection gives a short account, following Tanimura and Murayama,[32] Mukamel and co-workers,[31] and Domcke and Stock,[44] of the spectroscopic signal for pump−probe experiments in the impulsive limit. Against this background, we discuss the relevance to the experimental signal of the quantities observed in our simulations. Besides the excited-state populations, electronic coherence between the nonadiabatically coupled states is shown to contribute to the signal if both states have nonvanishing dipole moments with respect to the state accessed by the probe pulse.

4.2.1. Spectroscopic Signal: Impulsive Limit. The central quantity to be calculated in the context of a pump−probe experiment is the time-dependent polarization of the sample

induced by the probe pulse,[31,44] which reads as follows in the impulsive limit:[32,44]

$$P_{k_2}(t) = \mathrm{Im}[\mathrm{e}^{i\Omega_2\tau}\,\mathrm{Tr}\{\hat{\mu}_{ep}^{-}\,\hat{\rho}_{ep}(t)\}] \tag{17}$$

with a phase factor $\exp(i\Omega_2\tau)$ involving the carrier frequency Ω_2 of the probe pulse that is applied at time $t = \tau$, the dipole moment operator $\hat{\mu}_{ep} = \hat{\mu}_{ep}^{+} + \hat{\mu}_{ep}^{-} = \mu_{ep}(|e\rangle\langle p| + |p\rangle\langle e|)$, and the optical coherence $\hat{\rho}_{ep}(t)$. Here $|e\rangle$ represents the excited electronic state the evolution of which is to be monitored by the experiment, and $|p\rangle$ is the state accessed by the probe pulse. The latter coincides with the ground state $|g\rangle$ for a stimulated-emission process. In the above expression, the electromagnetic fields pertaining to the pump and probe pulses have been set to $E_{pump}(t) = \delta(t)$ and $E_{probe}(t) = \delta(t - \tau)$ for simplicity.

Different contributions to the optical coherence $\hat{\rho}_{ep}(t)$ may be distinguished. One contribution arises from populations $\hat{\rho}_{ee}$ that have previously evolved on the excited-state potential energy surface:[31,32,44]

$$\hat{\rho}_{ep}^{[ee]}(t) = \exp\{L_{mol}(t - \tau)\}\,[\hat{\rho}_{ee}(\tau)\hat{\mu}_{ep}^{+}] \tag{18}$$

where L_{mol} refers to the molecular Liouvillian including dissipation according to eq 4, but excluding the external field.

Another contribution, occurring along with stimulated emission in the case $|p\rangle = |g\rangle$ involves the part of the density operator that has remained in the electronic ground state prior to the probe pulse. This contribution is associated with a resonance Raman process that reduces to simple probe absorption from the stationary ground state $\hat{\rho}_{gg}$ in the impulsive limit:[31,32,44]

$$\hat{\rho}_{eg}^{[gg]}(t) = \exp\{L_{mol}(t - \tau)\}\,[\hat{\mu}_{eg}^{+}\rho_{gg}] \tag{19}$$

Still another contribution is to be expected for a curve-crossing scenario, in the case where both electronic states involved ($|e\rangle$ and $|f\rangle$) have nonvanishing dipole moments $\hat{\mu}_{ep}$ and $\hat{\mu}_{fp}$ with respect to the state $|p\rangle$:

$$\hat{\rho}_{ep}^{[ef]}(t) = \exp\{L_{mol}(t - \tau)\}\,[\hat{\rho}_{ef}(\tau)\hat{\mu}_{fp}^{+}] \tag{20}$$

The latter contribution can be understood as arising from *coherence transfer* between the electronic coherence $\hat{\rho}_{ef}$, generated by the coherent coupling between the states $|e\rangle$ and $|f\rangle$, and the coherence $\hat{\rho}_{ep}$ detected by the probe pulse. This contribution accompanies the "direct" one involving $[\hat{\rho}_{ff}(\tau)\hat{\mu}_{fp}^{+}]$, which is analogous to eq 18. These terms should be relevant if the probe field is nearly resonant with both states. The contribution of eq 20 apparently has not been considered in the literature so far.

All of the above contributions to the optical coherence $\hat{\rho}_{ep}(t)$ of course carry vibrational (or vibronic) populations and coherences. Since these can be characterized in terms of the complex eigenvalues of the Liouvillian, as shown in the preceding section, the Liouvillian spectrum eventually underlies the observable structures in a frequency-resolved pump−probe signal.

As pointed out by Domcke and Stock,[44] the diabatic, rather than adiabatic, populations are relevant to the observed signal, as may be inferred from a derivation using the Condon approximation.

5. Numerical Method

The present work uses a short-time propagation scheme for the numerical integration of the master equation, eq 4, in the coordinate representation. Since we do not consider the interaction with the electromagnetic field, the propagator is time-independent (but notice that the short-time propagation scheme can be easily extended to a time-dependent propagator),

$$U(\tau) = \exp\{(L_{coh} + L_{diss})\tau\} \tag{21}$$

with $L_{coh} = L_S$ and L_{diss} given by eq 10 in the coordinate representation. A "split-propagator" scheme is used, according to which[72,73]

$$U(\tau) = U_{coh}(\tau/2)U_{diss}(\tau)U_{coh}(\tau/2) + O(\tau^3) \tag{22}$$

which is valid in Liouville space like for ordinary Hilbert-space operators. The component propagators are given by $U_{coh}(\tau) = \exp\{L_{coh}\tau\} = \exp\{-i/\hbar(\mathcal{T} + V)\tau\}$ and $U_{diss}(\tau) = \exp\{L_{diss}\tau\}$. The coherent propagator is further split up, according to the same procedure:

$$U_{coh}(\tau) \sim U_{kin}(\tau/2)\,U_{pot}(\tau)\,U_{kin}(\tau/2) \tag{23}$$

with $U_{kin}(\tau) = \exp(-i/\hbar\mathcal{T}\tau)$ and $U_{pot}(\tau) = \exp(-i/\hbar V\tau)$. This is entirely analogous to the Hilbert-space procedure first proposed by Feit, Fleck, and Steiger.[72,73] The first application to density operator propagation in coordinate space was given by Hellsing and Metiu.[74]

Numerically, the overall propagation is thus composed of the following sequence:

$$U(n\tau) \sim U_{coh}(\tau/2)[U_{diss}(\tau)\,U_{coh}(\tau)]^n U^{\dagger}_{coh}(\tau/2) \tag{24}$$

where

$$U_{coh}(\tau) = U_{kin}\left(\frac{\tau}{2m}\right)\left[U_{pot}\left(\frac{\tau}{m}\right)U_{kin}\left(\frac{\tau}{m}\right)\right]^m U^{\dagger}_{kin}\left(\frac{\tau}{2m}\right) \tag{25}$$

with the possibility of introducing different time spacings for the potential/kinetic and coherent/relaxation parts of the propagator. This is convenient in cases where the higher-order commutator terms, which are neglected by the propagation method, are of greater importance (hence requiring smaller time steps) for the coherent as compared with the dissipative propagation steps.

The individual terms are calculated as follows, in the coordinate and momentum representations, respectively. For the potential-energy propagation step,

$$U_{pot}(r, r'; \tau)\,\boldsymbol{\rho}(r, r') = \exp\left(-\frac{i}{\hbar}\mathbf{V}(r)\tau\right)\boldsymbol{\rho}(r, r')\exp\left(\frac{i}{\hbar}\mathbf{V}(r')\tau\right) \tag{26}$$

where both $\mathbf{V}$ and $\boldsymbol{\rho}(r, r')$ represent 2×2 matrices in the basis of diabatic electronic states. Exponentiation of the potential matrix is carried out using the analytical expressions for a two-level system, as proposed in ref 75. The kinetic-energy step is performed in the momentum representation, in the same fashion for both electronic states,

$$U_{kin}(k, k'; \tau)\,\rho_{nm}(k, k') = \exp\left(-i\hbar\frac{k^2}{2\mu}\tau\right)\rho_{nm}(k, k')\exp\left(i\hbar\frac{k'^2}{2\mu}\tau\right) \tag{27}$$

The propagators may be grouped together as suggested in ref 74.

Finally, the evolution step under L_{diss} is carried out in the coordinate representation. The dissipative Liouvillian is set up

either in the diabatic or adiabatic representation, depending on which is more appropriate for the problem to be studied. If the adiabatic basis is chosen, the density operator is transformed accordingly before and after the dissipative propagation step, using the transformation eq 3. Alternatively, one might choose to transform the dissipative Liouvillian matrix between the adiabatic and diabatic representations.

The particular form of the dissipative Liouvillian of eq 10 is diagonal in a given pair of coordinates (r, r'), which is due to the fact that all of the Lindblad operators of eq 7 are local in coordinates. Notice that, if vibrational "friction" terms were to be included, this would no longer be the case, since those terms involve the form $[\hat{x}, [\hat{p},\hat{\rho}]_+]$, where $[\,]_+$ denotes an anticommutator.[58−61] In the particular case considered here, the 5×5 Liouvillian matrix $L_{\text{diss}}(r, r')$ of eq 10 may be diagonalized and exponentiated, such that $\exp\{L_{\text{diss}}(r, r')\tau\} = M^{\dagger} \exp\{L^{\text{diag}}_{\text{diss}}(r, r')\tau\}M$. In particular, the 3×3 block involving populations has to be diagonalized, while the 2×2 block for the coherences is already diagonal if the so-called nonsecular terms are disregarded.

Since the auxiliary state $|X\rangle$ is included only in the dissipative propagation step, it does not give rise to much additional numerical effort. The coordinate dependence of the rates $\Gamma_{X2}(r)$ may be chosen rather freely, for example, using a Gaussian envelope centered on the grid boundary, with a half-width of about 0.5 a_0. The principal requirement is that the coupling strength is large enough to allow for a complete "emission" once the coupling region is reached. By monitoring the norm (Tr ρ) of the state $|X\rangle$ along with the norm of the other states, one may numerically check on the conservation of the overall population under L_{diss}. As may be inferred from the matrix representation eq 10, the damping process due to the auxiliary state affects not only the electronic population of the dissociative state but also the electronic coherence between the states involved in the curve-crossing. In fact, the decay of electronic coherence has to be taken into account to assure the positivity of the diagonal elements of the density matrix. In the present model, where the other coherent and dissipative couplings are localized in the curve-crossing region, correlations between the "emission" process and the other interactions are not observed.

With the method described here, typical time intervals of $\Delta t = 0.5$ fs were used. The commutator terms which are neglected by the propagation scheme were calculated explicitly for this time interval and were shown to lie 2 orders of magnitude below the terms captured by the calculation. In fact, the propagation scheme turns out to be very robust in that it yields qualitatively correct results even if the commutator terms are nonnegligible. With a coordinate-space grid of 256 points, typical overall propagation times correspond to a few hours, on a workstation, for a time evolution over 1 ps. This evidently puts a limitation on the grid sizes that may be conveniently handled.

Finally, let us note that other ways of partitioning the overall Liouvillian are possible within a short-time propagation scheme. For example, the potential-energy part may be combined with the dissipative part. For other recent applications of short-time propagation schemes to density operator evolution, see refs 50, 51, 76, and 77.

6. Examples: Curve-Crossing with Dissipation

In the following, three different examples will be discussed that illustrate the effects of the dissipative time evolution on curve-crossing dynamics. The first example represents periodic Landau−Zener-type crossings with an initial condition on the upper adiabatic surface of the coupled potentials shown in Figure 1a. This situation closely resembles the one encountered in systems such as NaI.[6−8] The wavepacket shows recurrences in the upper adiabatic state, which are gradually damped by the loss of population each time the crossing is traversed. The second example corresponds to the same potential energy surfaces, but a different initial condition, which represents a coherent superposition of the adiabatic states. This example highlights the role of electronic, or vibronic, coherence. The third case corresponds to a model potential for I_2 (see Figure 1b), which has recently been applied in the analysis of the solvent-induced predissociation of the $B0_u^+$ state by Ben-Nun, Levine, and Fleming.[16] Here, we illustrate population transfer due to the indirect electronic coupling, in the absence of any coherent coupling. The example again shows a stepwise depletion of the electronic state initially populated, very similarly to the results obtained in the molecular dynamics approach by Ben-Nun et al.[16]

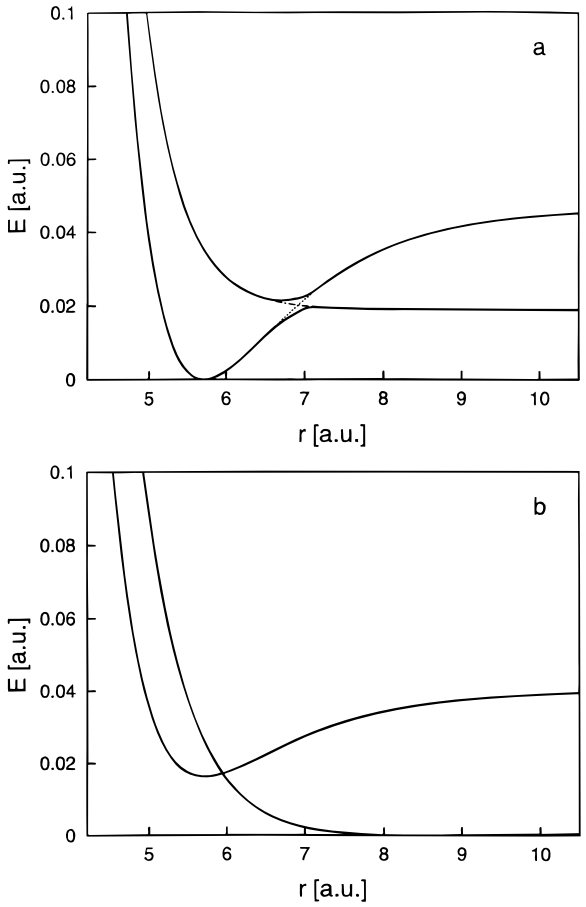

Figure 1. Two model potentials used in the present work. (a) Diabatic states are given by a Morse potential and an exponential form, respectively. For $V_1(r) = D_1[1 - \exp(-\beta_1(r - r_{10}))]^2$, the parameters are given by $D_1 = 0.0463$ *au*, $\beta_1 = 0.8975\ a_0^{-1}$, $r_{10} = 5.716\ a_0$, while for $V_2(r) = A_2 \exp(-\beta_2(r - r_{20})) + V_{20}$, the parameters are $A_2 = 0.02992$ *au*, $\beta_2 = 2.1590\ a_0^{-1}$, $r_{20} = 5.4235\ a_0$, and $V_{20} = 0.0189$ *au*. The diabatic coupling is chosen as $V_{12} = V_{12}^0 \exp(-[(r - r_X)/\sigma]^2)$ with $V_{12}^0 = 0.002$ *au*, $\sigma = 0.3\ a_0^{-1}$, and $r_X = 6.825\ a_0$. (b) Here, the diabatic states model the $B(0_u^+\ ^3\Pi)$ and $a(1_g\ ^3\Pi)$ states of I_2, with parameters adopted from Ben-Nun et al.[16] Notice that the dissociative potential features a very shallow well with a minimum at $r = 8.48\ a_0$.

Note that for all examples shown in the following, the reduced mass of iodine was used in the calculations. Further, all examples refer to a pure-state initial condition representing an excited-state wavepacket. The potential coupling between the diabatic states was chosen to be localized in space with a

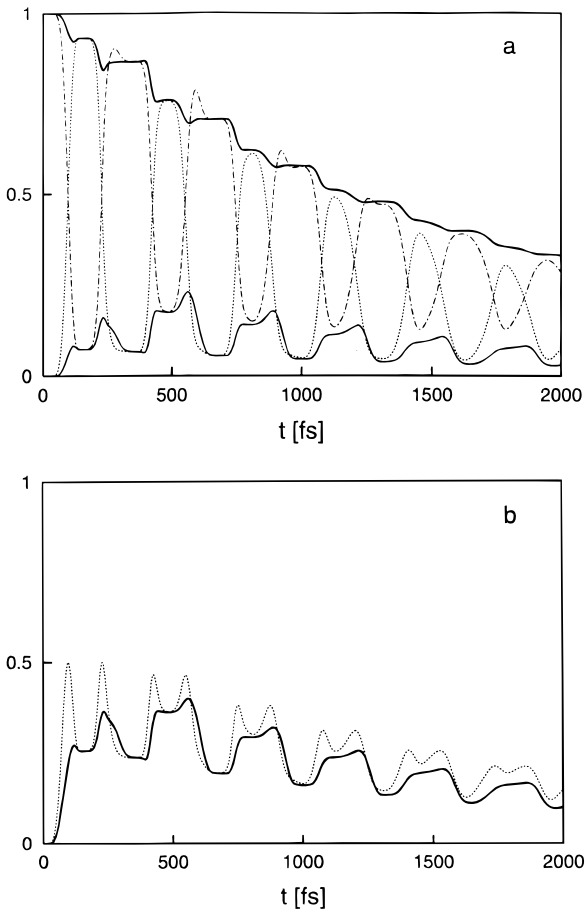

Figure 2. Time evolution of the integrated electronic populations and coherences, $|\rho_{mn}|(t)$ (see eq 16), for the first example system (see section 6.1.), without dissipation. The initial condition corresponds to a pure state $\rho(t_0) = |\psi(t_0)\rangle\langle\psi(t_0)|$, with $|\psi(t_0)\rangle$ representing a Gaussian wavepacket localized at $\langle r_0\rangle = 6.0\ a_0$, with width at half-height fwhm $= 0.15\ a_0$. (a) Electronic populations $|\rho_{nn}(t)|$, $n = 1, 2$, equal to $\mathrm{Tr}_r\{\rho_{nm}(t)\}$ for the pure-state case. Solid lines: adiabatic representation. Dotted and dash−dotted lines: diabatic representation. (b) Electronic coherences, $|\rho_{12}(t)| = |\rho_{21}(t)|$. Solid line: adiabatic representation. Dotted line: diabatic representation.

Gaussian envelope function. The detailed-balance condition eq 8 was applied for $T = 300$ K.

6.1. Periodic Level Crossings. For the first example, with an initial wavepacket localized at $\langle r_0\rangle \sim 6.0\ a_0$ on the upper adiabatic potential surface of Figure 1a, the time evolution of the integrated electronic populations and coherences in the adiabatic and diabatic representations is shown in Figure 2. It is clear that the adiabatic representation is more appropriate, while a complete population transfer between the diabatic states takes place each time the crossing is traversed. If we describe the population transfer by a simple model for repeated Landau−Zener-type transitions, we expect a stepwise exponential decay of the upper-state population, given approximately by $\exp[-P_{LZ}t/(T/2)]$ on stroboscopic monitoring at each half-period. This is confirmed by Figure 3, which shows the integrated population of the upper adiabatic state over an extended time interval (5 ps). With a wavepacket period of $T \sim 325$ fs in the upper state, we obtain the Landau−Zener transition probability $P_{LZ} \sim 0.09$. Figure 3 also shows the Hilbert-space correlation function in the diabatic representation, $|\langle\psi^{di}(t_0)\ \psi^{di}(t)\rangle|$, which is expected to trace out a decay envelope similar to the adiabatic populations, given that the resonances in the upper adiabatic state approximately decay with half-width $\Gamma = P_{LZ}/(T/2)$. (This result may be derived semiclassically from the properties of

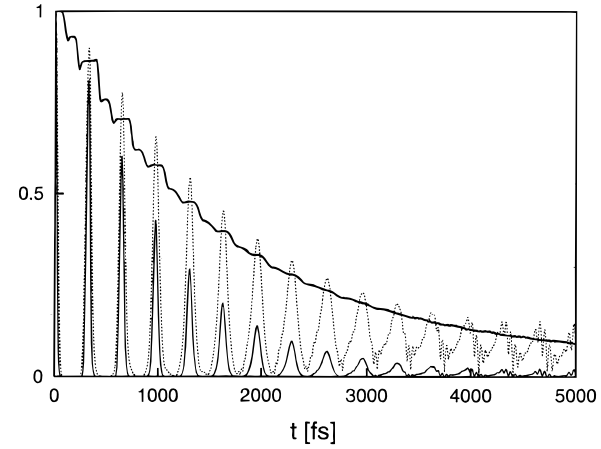

Figure 3. Same conditions as Figure 2. Upper solid line: integrated population of the upper adiabatic state, $|\rho^{ad}_{22}|(t)$. Dotted line: diabatic wavepacket correlation function (absolute value), $|\langle\psi^{di}_2(t_0)\ \psi^{di}_2(t)\rangle|$. Solid line: diabatic Liouvillian correlation function $C^{di}_{22}(t, t_0) = \mathrm{Tr}_r\{\rho^{di}_{22}(t_0)\ \rho^{di}_{22}(t)\}$, which is equal to $|\langle\psi^{di}_2(t_0)\ \psi^{di}_2(t)\rangle|^2$ for the pure-state case considered here. Note that the numerical agreement obtained between the wavepacket and density matrix calculations provides a convenient verification of the latter.

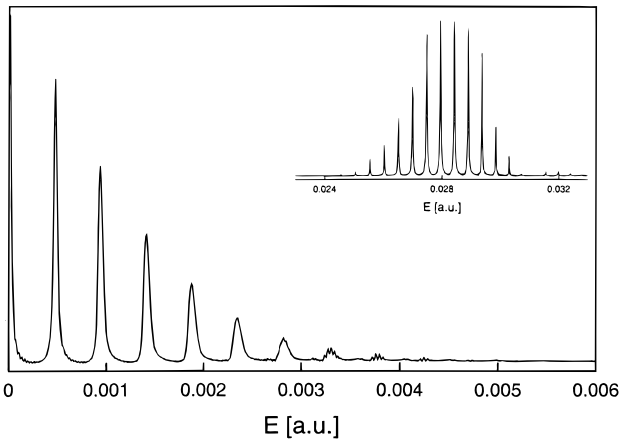

Figure 4. Liouville-space and Hilbert-space spectra. The central part of the figure shows the Fourier transform of the Liouvillian correlation function $C^{di}_{22}(t, t_0)$ of the preceding figure. The Fourier transform is symmetrical with respect to positive and negative frequencies, and only the positive-frequency part is shown here. Inset: Fourier transform (real part) of the wavepacket correlation function $\langle\psi^{di}_2(t_0)\ \psi^{di}_2(t)\rangle$. The Liouvillian spectrum displays differences of the energies given in the Hilbert-space spectrum.

the complex periodic orbit that alternates between the two surfaces.[71]) The Liouvillian correlation function is given by $C^{di}_{22}(t, t_0) = |\langle\psi^{di}_2(t_0)\ \psi^{di}_2(t)\rangle|^2$ for the isolated system. The Fourier transform of $C^{di}_{22}(t, t_0)$, shown in Figure 4, displays the vibrational coherences in the upper adiabatic state. Even though the generation of *electronic* coherence is central to the time evolution of the system, one does not observe discrete vibronic energy differences in the spectrum since continuum states, rather than bound states, of the lower adiabatic surface are involved.

The effects of dephasing and of "indirect" (environment-induced) electronic transitions are shown in Figure 5. The dissipative part of the Liouvillian has been calculated in the adiabatic representation, which is most appropriate to the present example. The decay constants are chosen to correspond to a time scale shorter than the decay with $\Gamma = P_{LZ}/(T/2)$, but longer than the Landau−Zener time scale $\tau_{LZ} \sim 50$ fs, which gives a measure of the time interval the wavepacket spends in the

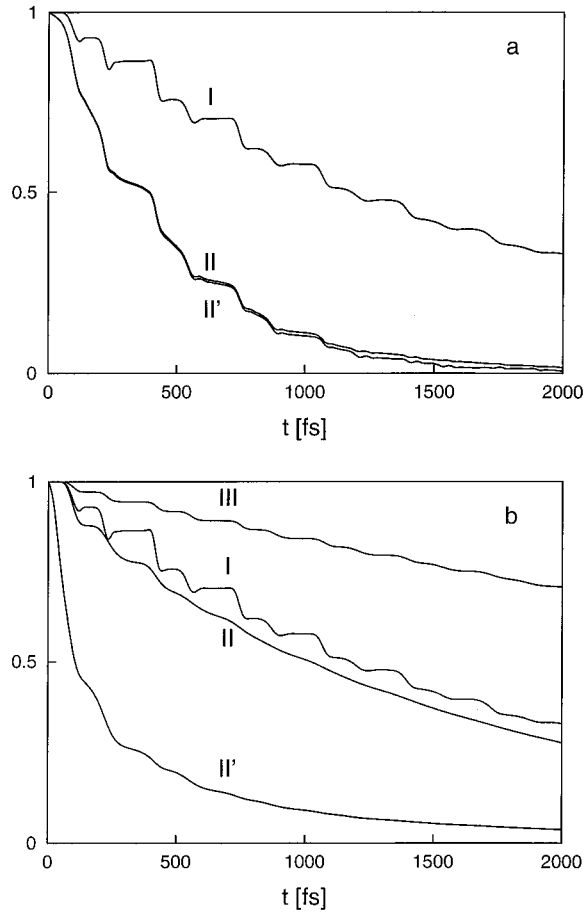

Figure 5. (a) Effects of "indirect" transitions on the population dynamics of the upper adiabatic surface. (I) Population decay without dissipation, reproduced from Figure 2. (II) Decay of $|\rho_{22}^{ad}|$ and (II′) of $\mathrm{Tr}_r\{\rho_{22}^{ad}\}$ in the presence of environment-induced transitions. The parameters $\Gamma_0 = 0.000075$ au and $\lambda = 0.01$ au determine the envelope function $\Gamma_{el}(r) = \Gamma_0/([\Delta V_{12}(r)/\lambda]^2 + 1)$, from which the rates $\Gamma_{12}(r)$ and $\Gamma_{21}(r)$ are derived in accordance with the detailed-balance condition eq 8. Note that $|\rho_{22}| = \mathrm{Tr}_r\{\rho_{22}\}$ for a pure-state wavepacket as given initially. (b) Effects of dephasing. (I) Dissipation-free case, as above. (II),(II′) $\mathrm{Tr}_r\{\rho_{22}^{ad}\}$ and $|\rho_{22}^{ad}|$, respectively, for vibrational dephasing with rates $\Gamma_{11,vib} = \Gamma_{22,vib} = 0.02$ au; r_1^0 and r_2^0 occurring in the dephasing operators correspond to the equilibrium positions of the adiabatic electronic states. The difference between $|\rho_{22}|$ and $\mathrm{Tr}\{\rho_{22}\}$ reflects the effect of "decoherence" that quickly destroys the initial vibrational pure state. (III) Electronic "pure dephasing", with rate $\Gamma_{11,el} = \Gamma_{22,el} = 0.1$ au, which quenches the Landau−Zener transitions and thus slows down the decay of the population $\mathrm{Tr}_r\{\rho_{22}^{ad}\}$ ($\mathrm{Tr}_r\{\rho_{22}^{ad}\} \simeq |\rho_{22}^{ad}|$ here).

crossing region. This time scale is given by $\tau_{LZ} = l_{LZ}/v = \Delta/v|F_2 - F_1|$,[50,64] where l_{LZ} denotes the width of the crossing region and $\Delta = 2|V_{12}(r_X)|$ is the energy gap between the adiabatic states. Figure 5 shows that the "indirect" transitions lead to a rapid depletion of the upper adiabatic state, while the lower state gains in population. Vibrational dephasing does not substantially affect the decay of $\mathrm{Tr}_r\{\rho_{22}^{ad}(t)\}$. However, "pure dephasing" of the electronic coherence that mediates the Landau−Zener type transitions may slow down the decay.

6.2. Vibronic versus Vibrational Coherence. The second example is chosen to illustrate under which circumstances electronic coherence can be observed in terms of discrete vibronic frequency components. The example refers to the same potential energy surface as above, but the initial condition now represents a coherent superposition of the adiabatic states centered around $\langle r_0 \rangle = 6.8\ a_0$, corresponding to an initial

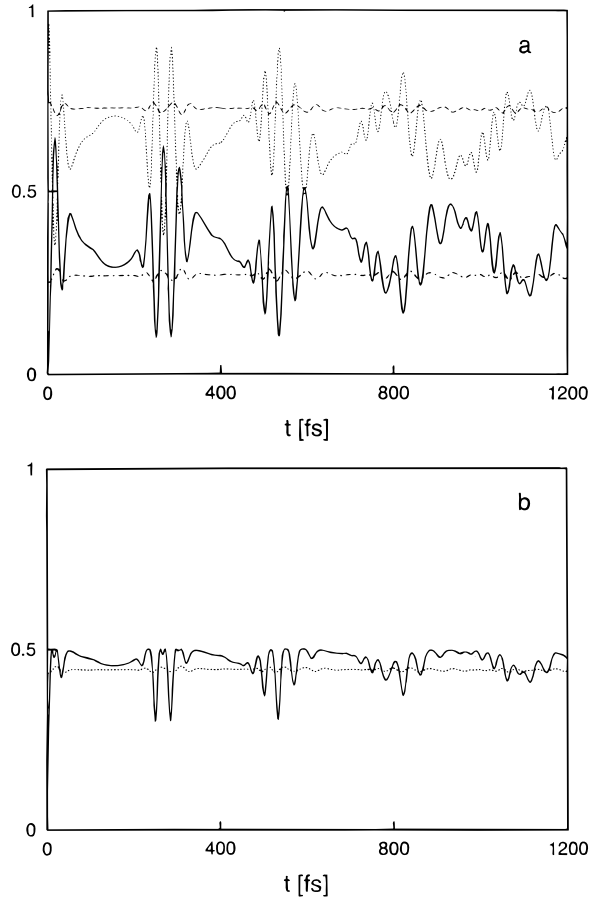

Figure 6. Time evolution of the integrated populations and coherences, $|\rho_{mn}|(t)$, for the second example system (see section 6.2.), without dissipation. The initial conditions are again given in terms of a pure state, which is now localized at $\langle r_0 \rangle = 6.8\ a_0$, with fwhm $= 0.15\ a_0$, on the dissociative diabatic surface, in the region of strong mixing between the diabatic states. Hence, this state represents a coherent superposition of electronic states in the adiabatic representation. (a) Populations $|\rho_{nn}|$, $n = 1,2$. Dashed and dash−dotted lines: adiabatic representation. Solid and dotted lines: diabatic representation. (b) Coherences $|\rho_{12}| = |\rho_{21}|$. Dotted line: adiabatic representation. Solid line: diabatic representation.

condition on the upper *diabatic* state in the region of strong state mixing. (As an alternative to the diabatic initial condition, one might choose a wavepacket in the adiabatic representation that covers the corresponding bandwidth. This, however, entails a strong participation of continuum states, which is avoided here for ease of interpretation.)

Figure 6 shows the integrated adiabatic and diabatic populations and coherences, in an analogous fashion to Figure 2. The state preparation is such that almost no perceptible decay occurs for the upper electronic state. This is due to the fact that only the lowest two vibrational levels of the upper-state manifold are accessed, which decay much more slowly than the higher vibrational levels that constitute the wavepacket of the first example.[71] From a semiclassical point of view, the upper-state preparation chosen here imparts very little kinetic energy to the wavepacket, which renders the semiclassical behavior strongly adiabatic. Considering the diabatic representation, notice that no complete swapping of populations takes place, as in the first example; we rather observe Rabi-type oscillations, with frequency components of the order of the electronic energy gap, whenever the crossing is traversed.

Figure 7a shows the Liouvillian spectrum obtained by Fourier-transforming the diabatic correlation function $C_{22}^{di}(t, t_0)$, along with the Hilbert-space spectrum. The contribution due to the

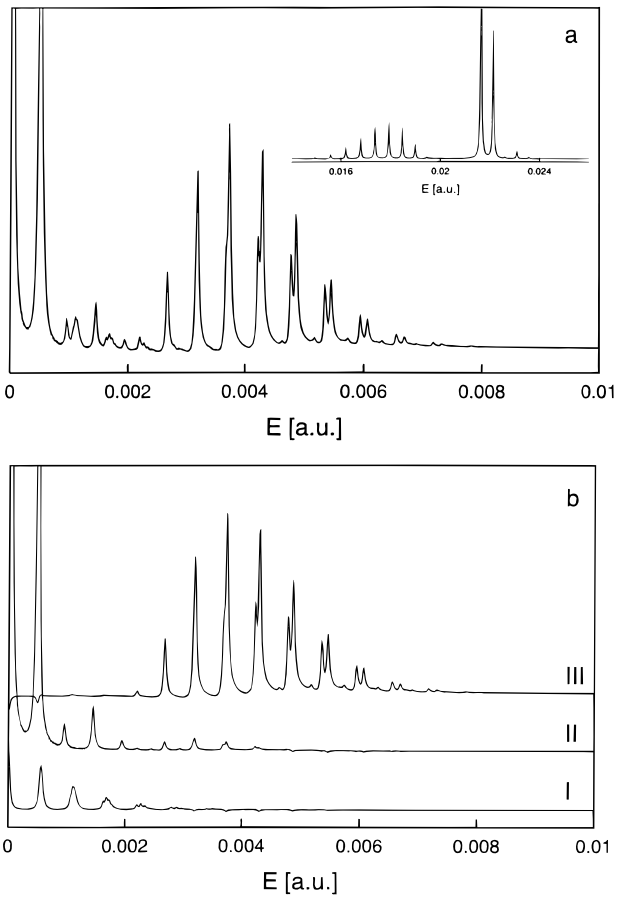

Figure 7. (a) Fourier transform of the Liouvillian correlation function $C_{22}^{di}(t, t_0)$ for the system described in the preceding figure. The correlation function (not shown here) was sampled over a time interval of 5 ps and shows barely any decay over this interval. The Fourier transform was obtained after suitable apodization. Inset: Hilbert-space spectrum obtained from wavepacket propagation. Notice that the initial condition samples the vibrational manifolds of both the upper and lower adiabatic states. Therefore, vibronic coherence is clearly distinct in the Liouvillian spectrum. (b) In contrast to part a, the Fourier transforms of the *adiabatic* correlation functions are shown: (I) Fourier transform of the correlation function for the lower adiabatic state, $C_{11}^{ad}(t, t_0)$; (II) Fourier transform of $C_{22}^{ad}(t, t_0)$; (III) Fourier transform of $C_{12}^{ad}(t, t_0)$. I and II display the *vibrational* coherence within the adiabatic electronic states, while III displays the *vibronic* coherence in the adiabatic basis.

vibronic coherence is clearly separated in the high-frequency part of the spectrum. This separation becomes even more transparent on considering the Fourier transforms of the adiabatic correlation functions, $C_{ij}^{ad}(t, t_0)$ in Figure 7b. For an experimental-state preparation similar to the one chosen here, vibronic coherence should thus be observable. For recent discussions on the issue of observability of electronic coherence, see refs 78 and 79. Figure 8 illustrates the effects of "indirect" transitions versus vibrational dephasing on the Liouvillian correlation function $C_{22}^{di}(t, t_0)$. The former effect again leads to a rapid depletion of the upper adiabatic state, whereas the latter tends to preserve the upper state population while exerting a damping on the vibrational (and electronic) coherence. Figure 9 shows the associated Liouvillian spectrum.

6.3. Environment-Induced Predissociation: Example I_2. The predissociation of I_2 in its $B0_u^+$ state has been subject to extensive experimental and theoretical investigation over the past few years. While the B state is very long-lived in the gas phase, the predissociation process is found to be extremely rapid in the condensed phase and in clusters. Scherer et al.,[3] using

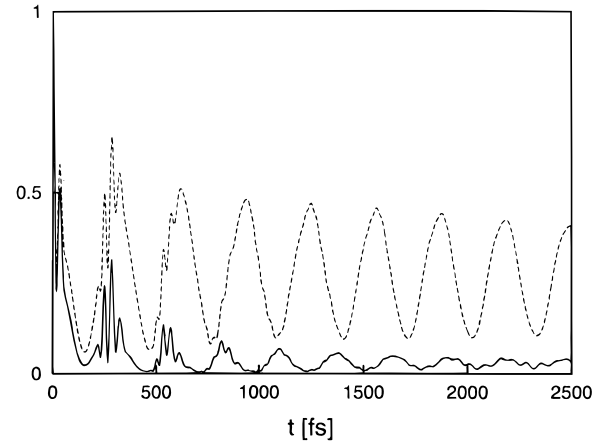

Figure 8. Liouvillian correlation functions $C_{22}^{di}(t, t_0)$ in the presence of "indirect" electronic transitions (solid line) and vibrational dephasing (dashed line). The rates are constructed as described in Figure 5, with $\Gamma_0 = 0.0002$ *au* and $\Gamma_{11,vib} = \Gamma_{22,vib} = 0.0001$ *au*. The decay of the upper adiabatic state is barely accelerated by the dephasing effect, such that oscillations persist for a much longer time than in the case where "indirect" transitions are involved.

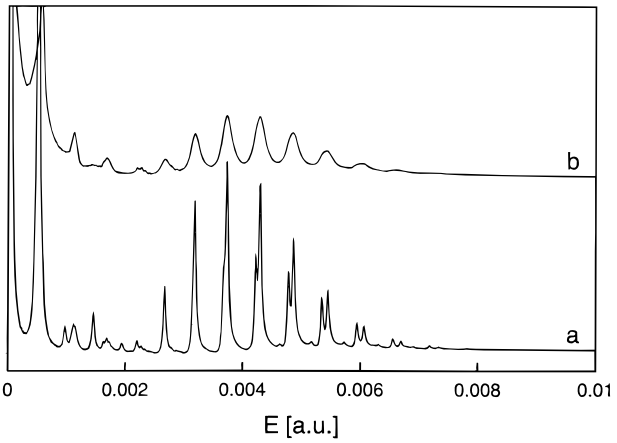

Figure 9. Fourier transform of $C_{22}^{di}(t, t_0)$ for the dissipation-free case (see Figure 7) as compared with the conditions of Figure 8 (both environment-induced transitions and dephasing lead to a similar "washing out" of the vibronic structure).

transient dichroism experiments, reported a decay within ~200 fs in liquid hexane, while Xu et al.[5] concluded on the grounds of resonance Raman experiments in CCl_4 that the process was even more rapid, on the order of 50 fs. Zewail and co-workers undertook a series of detailed investigations aimed at capturing the transition between gas-phase and liquid-phase dynamics.[1] For Ar and Kr as solvents, coherently oscillating signals are found at a pressure of 100 bar, but the coherence appears to be strongly quenched at 400 bar. For Ne and He, by contrast, an oscillatory transient signal persists for about 5 ps up to pressures of 2000 bar. Experiments on cryogenic matrixes were performed by Apkarian and co-workers,[4] who observed very long-lived coherent transients for I_2 embedded in a Kr matrix.

A number of theoretical interpretations have been suggested using, in particular, mixed quantum/classical approaches to the simulation of the combined solute-plus-solvent system.[13−16] By contrast, a "reduced-dynamics" treatment has not been proposed as yet. In this context, the purpose of the present contribution is not to give a detailed master equation analysis of the predissociation of I_2, but rather to point out that the approach presented here in principle accommodates the treatment of the solvent-induced dynamics. Recall from section 3 that the definition of the "indirect" electronic transitions is based on an

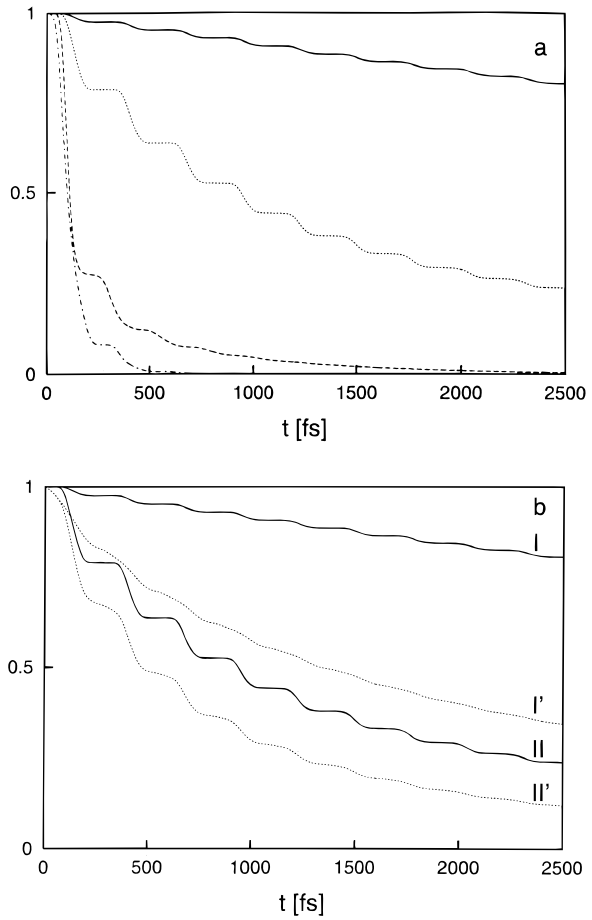

Figure 10. For the model potential of I_2 (Figure 1b), the populations of the diabatic states are shown, for nonvanishing effects of the "indirect" electronic transitions. The initial condition again corresponds to a pure state, localized at $\langle r_0 \rangle = 5.59\ a_0$, with a width fwhm $= 0.15\ a_0$. Notice that the dynamics does not involve any electronic coherence in this case. (a) Population of the bound diabatic state, $\mathrm{Tr}_r\{\rho_{11}^{\mathrm{di}}\}$, for parameters $\Gamma_0 = 0.00001$ au (solid line), $\Gamma_0 = 0.0001$ au (dotted line), $\Gamma_0 = 0.001$ au (dashed line), and $\Gamma_0 = 0.01$ au (dash−dotted line), respectively. The parameter which determines the coordinate dependence of the rates was chosen as above, $\lambda = 0.01$ au. Notice that $\mathrm{Tr}_r\{\rho_{11}^{\mathrm{di}}\} \simeq |\rho_{11}^{\mathrm{di}}|$ throughout. (b) Effects of vibrational dephasing. For $\Gamma_0 = 0.00001$ au (I) and $\Gamma_0 = 0.0001$ au (II) of the preceding figure, vibrational dephasing is added with rates $\Gamma_{11,\mathrm{vib}} = \Gamma_{22,\mathrm{vib}} = 0.002$ au (I′, II′) show $|\rho_{11}^{\mathrm{di}}|$, while$\mathrm{Tr}_r\{\rho_{11}^{\mathrm{di}}\}$ is barely affected by dephasing. The effect of "decoherence" is thus very similar to Figure 5b.

interaction Hamiltonian which is off-diagonal in the electronic states of the solute species. A detailed analysis, beyond the parametrization used in the present context, would entail (i) setting up the interaction Hamiltonian as a function of the intermolecular (and intramolecular) coordinates, for several dissociative states that intersect the $B0_u^+$ potential, and (ii) relaxing the Markovian assumption in the reduced-dynamics treatment, since a separation of time scales between the "system" and "bath" dynamics is not actually given. Thus, the present treatment, which assumes that electronic transitions are induced by rapid environmental fluctuations, can only offer a general perspective on the problem.

The potential energy surfaces shown in Figure 1b, representing the $B0_u^+$ and $a1_g$ states of iodine, are adopted from the work by Ben-Nun et al.[16] Figure 10 shows the integrated electronic population of the upper adiabatic state, for different values of the decay parameter associated with the "indirect" electronic transitions. The initial condition corresponds to a wavepacket centered on $\langle r_0 \rangle = 5.59\ a_0$ on the bound diabatic surface. The stepwise depletion of the initial state, as observed in Figure 10, is in correspondence with the results by Ben-Nun et al.[16] In contrast to the preceding examples, no electronic coherence is involved in the time evolution. Hence, a qualitative description may not be given in terms of the Landau−Zener model. (However, the Landau−Zener model may in principle be extended to include an imaginary coupling term that accounts for the indirect mechanism of population transfer.[47−49])

7. Discussion and Conclusions

The examples given above all refer to cases where the decay time scales are of the same order of magnitude, but somewhat longer than the coherent time scales characterizing the wavepacket motion, i.e., the wavepacket period $T \sim 300$ fs and the Landau−Zener time scale $\tau_{\mathrm{LZ}} \sim 50$ fs (see the first example). Hence, coherent motion is still observable, and the spectra associated with the complex eigenvalues of the Liouvillian show vibrational, or vibronic, structures. Notice that the frequency components occurring in such spectra are in direct correspondence with those observed in pump−probe spectra in the impulsive limit, as discussed in section 4.2. It might be interesting to extract explicitly the resonances underlying these spectra, which should yield lifetimes in the femto- to picosecond range. We have shown that in certain cases the vibrational and vibronic contributions to the spectrum may be clearly separated. The decay behavior observed in the above examples is not generally exponential. The simulations show that—as is to be expected—incoherent electronic transitions lead to a rapid depletion of the upper electronic state, while electronic "pure dephasing" may preserve the upper-state population for a longer time. Note, though, that conservation of the upper-state population may also be due to strong collisions that cause a substantial vibrational energy loss, as shown in recent work by Engel and co-workers on NaI.[12] This type of effect is not included in the present analysis.

The third example represents a simple model for environment-induced transitions of dissipative character, for a model representing the $B0_u^+$ and $a1_g$ states of I_2.[16] The population transfer via "indirect" transitions is very pronounced in this case since the crossing occurs close to the minimum of the bound-state potential well, which is very shallow. Recall that this example does not involve any electronic coherence. A more realistic treatment of this system, involving the investigation of the coupling Hamiltonian and the treatment of non-Markovian effects, is currently in progress in our group.

To summarize, the master equation approach presented in this work gives a qualitative picture of the influence that a dissipative environment may exert on a predissociation process. We have focused on examples illustrating the role of dephasing and of indirect (or incoherent) electronic coupling. The latter effect has not been considered so far in the majority of studies on curve-crossing processes including dissipation,[20−24] but it is related to recent investigations of the effect of spontaneous emission on Landau−Zener-type transitions in quantum optics.[50−52] In the Markovian limit, the decay of coherences and populations may be described by an appropriate parametrization, which is here accommodated in the framework of a master equation of Lindblad type. The choice of parameters reflects different time scales of evolution, which are fundamentally associated with the decay modes given by the complex eigenvalues of the Liouvillian. These should be compared with the "semiclassical" time scales associated with wavepacket motion to interpret the observations by time-resolved spectroscopy. Notice that the length scales associated with the wave-

packet are also important in defining vibrational dephasing in the coordinate representation.

The numerical approach presented in this work is based on a short-time propagation scheme that represents a viable alternative to other density-matrix propagation methods in coordinate space, in particular, the global propagation schemes introduced by Kosloff and co-workers.[33,34] The problem of defining "absorbing boundaries" to avoid reflections due to the finite extension of the coordinate-space grid has been solved by introducing an emission process to an auxiliary state, localized near the grid boundary. This method turns out to be very robust and represents an alternative to the use of the Wigner representation in defining the behavior of the density matrix at the boundary.[32]

Finally, let us remark that a more microscopic treatment of the ultrafast decay processes under consideration would entail taking into account non-Markovian effects, which should capture the actual solute−solvent dynamics that evolves between the static ("inhomogeneous") limit and the Markovian limit of rapid fluctuations. It is planned to extend the present study to the non-Markovian case, which should allow an interesting comparison with recent work by Tanimura and Murayama[32] as well as Coalson and co-workers.[28]

Acknowledgment. We would like to thank the organizers of the Femtochemistry 1997 conference for kindly inviting us to contribute to this special issue. Special thanks are due to Herbert Rotscheidt for his help in optimizing the performance of the program for density matrix propagation used in this work. Stephan Wefing contributed much advice and patience during the preparation of the manuscript. The author is very grateful to Peter Saalfrank for an introduction to other methods of density operator propagation and for valuable discussions that showed the analogies between the problem treated in this paper and earlier work on photodesorption from surfaces. Further, helpful discussions with Christian Kunz and Bernd Hess on the ab initio aspects of the "reduced-dynamics" problem are acknowledged. Vincent Brems pointed out refs 49 and 70 to the author. Many thanks are also due to Pierre Gaspard for numerous discussions in the early phase of this project and, in particular, for introducing the author to the relevance of short-lived resonances in Hilbert space and Liouville space. Finally, a fellowship of the Deutsche Forschungsgemeinschaft (DFG) is gratefully acknowledged.

Appendix. "Indirect" Transitions: Redfield Equations

In this Appendix, we consider a simple approach to the "indirect" electronic transitions via the Redfield equations, i.e., using a master equation of the type

$$\frac{\mathrm{d}}{\mathrm{d}t}\hat{\rho}_\mathrm{S} = \mathcal{L}_\mathrm{S}\hat{\rho}_\mathrm{S} + \mathcal{L}_\mathrm{diss}\hat{\rho}_\mathrm{S} = -\frac{\mathrm{i}}{\hbar}[\hat{H}_\mathrm{S}, \hat{\rho}_\mathrm{S}] - \frac{1}{\hbar^2}\int_0^\infty \mathrm{d}\tau\, \mathrm{Tr}_\mathrm{B}\{[\hat{H}_\mathrm{SB}, [\hat{H}_\mathrm{SB}(-\tau), \hat{\rho}_\mathrm{B}^\mathrm{ref}\hat{\rho}_\mathrm{S}(t)]]\} \quad (28)$$

where $\hat{H}_\mathrm{SB}(-\tau)$ is the Heisenberg operator,

$$\hat{H}_\mathrm{SB}(-\tau) = \exp(\mathcal{L}_0\tau)\hat{H}_\mathrm{SB} = \exp\left(-\frac{\mathrm{i}}{\hbar}\hat{H}_0\tau\right)\hat{H}_\mathrm{SB}\exp\left(\frac{\mathrm{i}}{\hbar}\hat{H}_0\tau\right) \quad (29)$$

and $\hat{\rho}_\mathrm{B}^\mathrm{ref}$ is a reference state for the environment, usually representing thermal equilibrium. We consider the following interaction Hamiltonian:

$$\hat{H}_\mathrm{SB} = \sum_n v_n(\hat{s}_+ a_n + \hat{s}_- a_n^\dagger) \quad (30)$$

where $\hat{s}_+ = |2\rangle\langle 1|$ and $\hat{s}_- = |1\rangle\langle 2|$ represent level-shift operators for the electronic levels of the molecule, while a_n and $a_n^\dagger$ are bosonic annihilation and creation operators for the bath which is modeled in terms of a collection of harmonic oscillators, $\hat{H}_\mathrm{B} = \sum_n k_n a_n^\dagger a_n$. The "unperturbed" Hamiltonian is given by $\hat{H}_0 = \hat{H}_\mathrm{S} + \hat{H}_\mathrm{B}$, and the associated Liouvillian $\mathcal{L}_0$ is defined accordingly. The rotating-wave approximation is made here, implying that only resonant terms contribute to the interaction.[80]

As an alternative form for the interaction Hamiltonian one may choose $\hat{H}_\mathrm{SB} = (\hat{s}_+ + \hat{s}_-)\hat{b}(\mathbf{r}_\mathrm{inter})$, where $\mathbf{r}_\mathrm{inter}$ collectively denotes the relative coordinates between the diatomic and the environment species. Note that both forms of the Hamiltonian imply that fluctuations in the "bath" coordinates $\mathbf{r}_\mathrm{inter}$ give rise to electronic transitions via the level-shift operators for the "system". The two model Hamiltonians have in common their independence of the vibrational coordinate of the diatomic, such that vibrational dephasing and relaxation are disregarded in the present considerations. In the following, we will focus on the form of the Hamiltonian given in eq 30, since this form yields the detailed-balance condition of eq 8 in the most transparent fashion.

Substitution of eq 30 into eq 28 yields for the dissipative part of the master equation

$$\mathcal{L}_\mathrm{diss}\hat{\rho}_\mathrm{S} = -\frac{1}{\hbar^2}\int_0^\infty \mathrm{d}\tau \sum_n v_n{}^2 \left\{ \frac{\exp(-\mathrm{i}k_n\tau/\hbar)}{[1-\exp(-\beta k_n)]}[\hat{s}_+, \hat{s}_-(-\tau)\hat{\rho}_\mathrm{S}] - \frac{\exp(\mathrm{i}k_n\tau/\hbar)}{[1-\exp(-\beta k_n)]}[\hat{s}_-, \hat{\rho}_\mathrm{S}\hat{s}_+(-\tau)] - \frac{\exp(-\mathrm{i}k_n\tau/\hbar)}{[\exp(\beta k_n)-1]}[\hat{s}_+, \hat{\rho}_\mathrm{S}\hat{s}_-(-\tau)] + \frac{\exp(\mathrm{i}k_n\tau/\hbar)}{[\exp(\beta k_n)-1]}[\hat{s}_-, \hat{s}_+(-\tau)\hat{\rho}_\mathrm{S}] \right\} \quad (31)$$

where the following relations for harmonic oscillators were used: $\mathrm{Tr}_\mathrm{B}\{a_n a_n^\dagger \hat{\rho}_\mathrm{B}^\mathrm{eq}\} = 1/[1-\exp(-\beta k_n)]$ and $\mathrm{Tr}_\mathrm{B}\{a_n^\dagger a_n \hat{\rho}_\mathrm{B}^\mathrm{eq}\} = 1/[\exp(\beta k_n)-1]$, with the equilibrium density operator $\hat{\rho}_\mathrm{B}^\mathrm{eq} = \exp(-\beta\hat{H}_\mathrm{B})/\prod_n[1-\exp(-\beta k_n)]^{-1}$, where the denominator represents the partition function, and $\beta = 1/(kT)$.[18]

While the evaluation of the Heisenberg operators $\hat{s}_\pm(-\tau)$ is straightforward in the representation of eigenstates of the "system" Hamiltonian, it is more involved in the coordinate representation. However, in the particular case we are considering, with the interaction Hamiltonian being independent of the "system" nuclear coordinate, we can derive a simple result for the Heisenberg operator, which depends only on the potential energy gap between the two electronic states at a given internuclear distance r_S. We assume here that $\hat{H}_\mathrm{S}$ is diagonal in the electronic states 1 and 2 (as well as in the kinetic-energy contribution),

$$\hat{H}_\mathrm{S} = \sum_{n=1,2}\hat{h}_n(r_\mathrm{S})|n\rangle\langle n| = \sum_{n=1,2}\{\hat{T}_n + \hat{V}_n(r_\mathrm{S})\}|n\rangle\langle n| \quad (32)$$

Hence, we have, for example, for $\hat{s}_+ = |2\rangle\langle 1|$,

$$\hat{s}_+(-\tau) = [\exp(L_S\tau)]_{21,21}|2\rangle\langle 1| = \exp\left(-\frac{i}{\hbar}\hat{h}_2\tau\right)|2\rangle\langle 1|\exp\left(\frac{i}{\hbar}\hat{h}_1\tau\right) \quad (33)$$

and an analogous expression for $\hat{s}_-(-\tau)$. The relevant elements of the Liouvillian propagator may be denoted "coherence Green function".[31] To introduce the dependence on the electronic energy gap, $\Delta V_{12}(r_S) = [V_1(r_S) - V_2(r_S)]$, the propagator for the individual electronic states, $\exp(-(i/\hbar)\hat{h}_n t)$, may be expressed in terms of the propagator for a chosen reference Hamiltonian $\hat{h}_{ref}$ (of the same structure as the $\hat{h}_n$'s) and an interaction-frame propagator involving $\Delta V_{n,ref}(r_S) = [V_n(r_S) - V_{ref}(r_S)]$,[31]

$$\exp\left(-\frac{i}{\hbar}\hat{h}_n t\right) = \exp\left(-\frac{i}{\hbar}\hat{h}_{ref}t\right)\exp_+\left[-\frac{i}{\hbar}\int_0^t dt'\,\Delta V_{n,ref}(r_S;t')\right] \quad (34)$$

where "$\exp_+$" denotes the (positive) time-ordered exponential.

In particular, the Hamiltonian $\hat{h}_1$ (or, equivalently, $\hat{h}_2$) may be chosen as the reference Hamiltonian to yield, for example, for an operator of the form $\hat{h}_+ = \hat{h}_{nuc}(r_S)|2\rangle\langle 1|$:

$$\hat{h}_+(t) = |2\rangle\langle 1|\exp\left(\frac{i}{\hbar}\hat{h}_2 t\right)\hat{h}_{nuc}(r_S)\exp\left(-\frac{i}{\hbar}\hat{h}_2 t\right)\times \exp_+\left[-\frac{i}{\hbar}\int_0^t dt'\,\Delta V_{12}(r_S;t')\right] \quad (35)$$

For the particular case of the operators $\hat{s}_\pm$ considered above, which do not depend on the nuclear coordinate r_S, we simply obtain

$$\hat{s}_+(t) = |2\rangle\langle 1|\exp_+\left[-\frac{i}{\hbar}\int_0^t dt'\,\Delta V_{12}(r_S;t')\right] \quad (36)$$

Since the time interval contributing to the integral over the Markovian kernel of eq 28 is on the order of the correlation time of the environment, τ_c (supposed to be substantially shorter than the time scale of "system" evolution), we may approximate $\Delta V_{12}(r_S;t') \sim \Delta V_{12}(r_S)$, such that

$$\exp_+\left[-\frac{i}{\hbar}\int_0^t dt'\,\Delta V_{12}(r_S;t')\right] \sim \exp\left[-\frac{i}{\hbar}t\Delta V_{12}(r_S)\right] \quad (37)$$

This expression is a *local* operator in the coordinate representation, and hence, the Heisenberg operator occurring in the master equation is local in coordinate space as well, $\hat{s}_+(-\tau) = \hat{s}_+ \exp[i\tau\Delta V_{12}(r_S)/\hbar]$. The master equation thus reads

$$L_{diss}\hat{\rho}_S(r_S, r'_S) = -\frac{1}{\hbar^2}\{J_{12}(r_S)[\hat{s}_+, \hat{s}_-\hat{\rho}_S(r_S, r'_S)] - J_{12}(r'_S)[\hat{s}_-, \hat{\rho}_S(r_S, r'_S)\hat{s}_+] - J_{21}(r'_S)[\hat{s}_+, \hat{\rho}_S(r_S, r'_S)\hat{s}_-] + J_{21}(r_S)[\hat{s}_-, \hat{s}_+\hat{\rho}_S(r_S, r'_S)]\} \quad (38)$$

where the spectral densities J_{12} and J_{21} depend on the energy gap at a given internuclear distance r_S,

$$J_{12}(r_S) = \mathrm{Re}\int_{-\infty}^{\infty} dk\,\frac{g(k)}{[1-\exp(-\beta k)]}\times \int_0^\infty d\tau\,\exp\left(-\frac{i}{\hbar}[k - \Delta V_{21}(r_S)]\tau\right) = \frac{g(\Delta V_{21}(r_S))}{[1-\exp(-\beta\Delta V_{21}(r_S))]}$$

$$J_{21}(r_S) = \frac{g(\Delta V_{21}(r_S))}{[\exp(\beta\Delta V_{21}(r_S)) - 1]} \quad (39)$$

Here, the sum over bath oscillators was replaced by an integral involving a strength function, $\sum_n \nu_n^2 \rightarrow g(k)$, and the time integral was carried out formally, $\int_0^\infty d\tau\,\exp[-i(k - \Delta V_{12}(r_S))\tau/\hbar] = \delta(k - \Delta V_{12}(r_S)) + iP\int dk/(k - \Delta V_{12}(r_S))$, where the last term represents a principal-value integral. For details of this procedure, see, e.g., reference 18. Notice that the principal-value term generates a frequency shift that is not taken into consideration here. The ratio of the rates $J_{12}(r_S)$ and $J_{21}(r_S)$ yields the detailed-balance condition eq 8.

For the alternative choice of the interaction Hamiltonian, $\hat{H}_{SB} = (\hat{s}_+ + \hat{s}_-)\hat{b}(\mathbf{r}_{inter})$ (see above), it is convenient to consider the classical-limit time correlation function $C(\tau) = \langle b^{cl}(\tau)\, b^{cl}(0)\rangle$, the Fourier transform of which yields the distribution $g(k)$. The latter has to be supplemented by the thermal factors occurring in eqs 31 and 39, to yield the correct ratio between "up" and "down" rates. For an exponentially decaying correlation function, $C(\tau) \sim \exp(-\tau/\tau_c)$, where τ_c is the correlation time of fluctuations in $b(\mathbf{r}_{inter})$, a Lorentzian spectral density is obtained, $g(k) \sim g_0(1/\tau_c)^2/[k^2 + (1/\tau_c)^2]$. This is the form chosen for the transition rates in the Lindblad form, with $\lambda = 1/\tau_c$ (see section 3.2).

If we equate the spectral densities J_{12} and J_{21} with the rates Γ_{12} and Γ_{21} associated with the Lindblad operators $\hat{C}_{12,el}$ and $\hat{C}_{21,el}$, it turns out that the terms represented by $\sum_i -(1/2)(\hat{C}_i^\dagger\hat{C}_i\hat{\rho}_S + \hat{\rho}_S\hat{C}_i^\dagger\hat{C}_i)$ agree with the corresponding terms in the Redfield equations, while those given by $\sum_i\hat{C}_i\hat{\rho}_S\hat{C}_i^\dagger$ disagree as far as the dependence on r_S and r'_S is concerned. The matrix representation of the Redfield form is given by

$$L_{diss}(r, r') = \frac{1}{\hbar^2}\times\begin{pmatrix} -\frac{1}{2}\{J_{21}(r)+J_{21}(r')\} & \frac{1}{2}\{J_{12}(r)+J_{12}(r')\} & 0 & 0 \\ \frac{1}{2}\{J_{21}(r)+J_{21}(r')\} & -\frac{1}{2}\{J_{12}(r)+J_{12}(r')\} & 0 & 0 \\ 0 & 0 & -\frac{1}{2}\{J_{21}(r)+J_{12}(r')\} & 0 \\ 0 & 0 & 0 & -\frac{1}{2}\{J_{21}(r')+J_{12}(r)\} \end{pmatrix} \quad (40)$$

Numerical implementation shows that the results given by the Lindblad versus Redfield form are very similar, but slightly negative values may indeed occur for the diagonal elements of the density operator evolving according to the Redfield form.

Finally, recall that the interaction Hamiltonian of eq 30 takes into account only the resonant interactions; that is, terms of the form $\hat{s}^{+}a_n^{\dagger}$ and $\hat{s}a_n$ have been omitted, in accordance with the "rotating-wave approximation".[80,81] However, these "nonsecular" terms[27,41,80−81] may be of importance if the unperturbed states are separated by small energy differences. Hence, we have included these terms in the master equation and conclude from the numerical result that they do not have a substantial influence on the time evolution of the systems considered here. The nonsecular terms are not compatible with the Lindblad form and, in fact, can yield "negative probabilities" in our simulations.

References and Notes

(1) Lienau, C.; Zewail, A. H. *J. Phys. Chem.* **1996**, *100*, 18629. Materny, A.; Lienau, C.; Zewail, A. H. *J. Phys. Chem.* **1996**, *100*, 18650. Liu, Q.; Wan, C.; Zewail, A. H. *J. Phys. Chem.* **1996**, *100*, 18666.

(2) Lienau, C.; Williamson, J. C.; Zewail, A. H. *Chem. Phys. Lett.* **1993**, *213*, 289.

(3) Scherer, N. F.; Jonas, D. M.; Fleming, G. R. *J. Chem. Phys.* **1993**, *99*, 153.

(4) Zadoyan, R.; Sterling, M.; Apkarian, V. A. *J. Chem. Soc. Faraday Trans.* **1996**, *92*, 1821.

(5) Xu, J.; Schwentner, N.; Chergui, M. *J. Chem. Phys.* **1994**, *101*, 7381. Xu, J.; Schwentner, N.; Hennig, S.; Chergui, M. *J. Chim. Phys.* **1995**, *92*, 541.

(6) Knopp, G.; Schmitt, M.; Materny, A.; Kiefer, W. *J. Phys. Chem. A* **1997**, *101*, 4852.

(7) Rosker, M. J.; Rose, T. S.; Zewail, A. H. *Chem. Phys. Lett.* **1988**, *146*, 175. Rose, T. S.; Rosker, M. J.; Zewail, A. H. *J. Chem. Phys.* **1989**, *91*, 7415. Cong, P.; Roberts, G.; Herek, J. L.; Mohktari, A.; Zewail, A. H. *J. Phys. Chem.* **1996**, *100*, 7832.

(8) Engel, V.; Metiu, H. *J. Chem. Phys.* **1989**, *90*, 6116; *J. Chem. Phys.* **1989**, *91*, 1596.

(9) Wan, C.; Gupta, M.; Zewail, A. H. *Chem. Phys. Lett.* **1996**, *256*, 279. Helbing, J.; Ciulin, V.; Portella-Oberli, M.; Chergui, M. In preparation.

(10) Wang, Q.; Schoenlein, R. W.; Peteanu, L. A.; Mathies, R. A.; Shank, C. V. *Science* **1994**, *266*, 422.

(11) Vos, M. H.; Rappaport, F.; Lambry, J.-C.; Breton, J.; Martin, J.-L. *Nature* **1993**, *363*, 320.

(12) Dietz, H.; Knopp, G.; Materny, A.; Engel, V. *Chem. Phys. Lett.* **1997**, *275*, 519.

(13) Batista, V. S.; Coker, D. F. *J. Chem. Phys.* **1996**, *105*, 4033; *J. Chem. Phys.* **1997**, *106*, 6923.

(14) Jungwirth, P.; Fredj, E.; Gerber, R. B. *J. Chem. Phys.* **1996**, *104*, 9332.

(15) Fang, J.-Y.; Martens, C. C. *J. Chem. Phys.* **1996**, *104*, 3684. Li, Z.; Fang, J.-Y.; Martens, C. C. *J. Chem. Phys.* **1996**, *104*, 6919.

(16) Ben-Nun, M.; Levine, R. D.; Fleming, G. R. *J. Chem. Phys.* **1996**, *105*, 3035.

(17) Fick, E.; Sauermann, G. *The Quantum Statistics of Dynamic Processes*; Springer: Berlin, 1990.

(18) Van Kampen, N. G., *Stochastic Processes in Physics and Chemistry*; Elsevier Science Publishers: Amsterdam, 1992.

(19) Spohn, H. *Rev. Mod. Phys.* **1980**, *53*, 569.

(20) Jean, J. M. *J. Chem. Phys.* **1994**, *101*, 10464. Jean, J. M.; Fleming, G. R. *J. Chem. Phys.* **1995**, *103*, 2092. Jean, J. M. *J. Chem. Phys.* **1996**, *104*, 5638.

(21) Hayashi, M.; Yang, T.-S.; Mebel, A.; Chang, C. H.; Lin, S. H.; Scherer, N. F. *Chem. Phys.* **1997**, *217*, 259.

(22) May, V.; Kühn, O.; Schreiber, M. *J. Phys. Chem.* **1993**, *97*, 12591. Kühn, O.; May, V. *Chem. Phys. Lett.* **1994**, *225*, 511. Kühn, O.; May, V.; Schreiber, M. *J. Chem. Phys.* **1994**, *101*, 10404.

(23) Wolfseder, B.; Domcke, W. *Chem. Phys. Lett.* **1995**, *235*, 370, **1996**, *259*, 113. Wolfseder, B.; Seidner, L.; Domcke, W. *Chem. Phys.* **1997**, *217*, 275.

(24) Tanimura, Y.; Mukamel, S. *J. Chem. Phys.* **1994**, *101*, 3049.

(25) Basilevsky, M. V.; Voronin, A. I. *J. Chem. Soc. Faraday Trans.* **1997**, *93*, 989.

(26) Bixon, M.; Jortner, J. *J. Chem. Phys.* **1997**, *107*, 1470.

(27) Coalson, R. D.; Evans, D. G.; Nitzan, A. *J. Chem. Phys.* **1994**, *101*, 436.

(28) Evans, D. G.; Coalson, R. D. *J. Chem. Phys.* **1993**, *99*, 6264; **1994**, *100*, 5605; **1995**, *102*, 5658.

(29) Cho, M.; Silbey, R. J. *J. Chem. Phys.* **1995**, *103*, 595.

(30) Lami, A.; Santoro, F. *J. Chem. Phys.* **1997**, *106*, 94.

(31) Mukamel, S., *Principles of Nonlinear Optical Spectroscopy*; Oxford University Press: New York/Oxford, 1995.

(32) Tanimura, Y.; Maruyama, Y. *J. Chem. Phys.* **1997**, *107*, 1779.

(33) Berman, M.; Kosloff, R.; Tal-Ezer, H. *J. Phys. A* **1992**, *25*, 1283.

(34) Kosloff, R. *Annu. Rev. Phys. Chem.* **1994**, *45*, 145.

(35) Banin, U.; Bartana, A.; Ruhman, S.; Kosloff, R. *J. Chem. Phys.* **1994**, *101*, 8461.

(36) Saalfrank, P.; Kosloff, R. *J. Chem. Phys.* **1996**, *105*, 2441.

(37) Saalfrank, P.; Baer, R.; Kosloff, R. *Chem. Phys. Lett.* **1994**, *230*, 463.

(38) Alicki, R.; Lendi, K. *Quantum Dynamical Semigroups and Applications*; Springer: Berlin, 1987.

(39) Lindblad, G. *Commun. Math. Phys.* **1976**, *48*, 119. Gorini, V.; Kossakowski, A.; Sudarshan, E. C. G. *J. Math. Phys.* **1976**, *17*, 821.

(40) Kosloff, R.; Ratner, M. A.; Davis, W. B. *J. Chem. Phys.* **1997**, *106*, 7036.

(41) Redfield, A. G. *IBM J. Res. Develop.* **1957**, *1*, 19; *Adv. Magn. Reson.* **1965**, *1*, 1.

(42) Pollard, W. T.; Friesner, R. A. *J. Chem. Phys.* **1994**, *100*, 5054.

(43) Walsh, A. M.; Coalson, R. D. *Chem. Phys. Lett.* **1992**, *198*, 293.

(44) Domcke, W.; Stock, G. *Adv. Chem. Phys.* **1997**, *100*, 1.

(45) Stock, G.; Schneider, R.; Domcke, W. *J. Chem. Phys.* **1989**, *90*, 7184.

(46) Sidis, V. *Adv. Chem. Phys.* **1992**, *82*, 73. Pacher, T.; Cederbaum, L. S.; Köppel, H. *Adv. Chem. Phys.* **1993**, *84*, 293. Parlant, G.; Yarkony, D. R. *Int. J. Quantum Chem.* **1992**, *26*, 737.

(47) Sidis, V.; Grimbert, D.; Courbin-Gaussorgues, C. *J. Phys. B.* **1988**, *21*, 2879.

(48) Devdariani, A. Z.; Ostrovskii, V. N.; Sebyakin, Yu. N. *Sov. Phys. JETP* **1976**, *44*, 477.

(49) Makhmetov, G. E.; Borisov, A. G.; Teillet-Billy, D.; Gauyacq, J. P. *Europhys. Lett.* **1994**, *27*, 247.

(50) Lai, W. K.; Suominen, K.-A.; Garraway, B. M.; Stenholm, S. *Phys. Rev. A* **1993**, *47*, 4779.

(51) Garraway, B. M.; Suominen, K.-A. *Rep. Prog. Phys.* **1995**, *58*, 365.

(52) Akulin, V. M.; Schleich, W. P. *Phys. Rev. A* **1992**, *46*, 4110.

(53) Zwanzig, R. *J. Chem. Phys.* **1960**, *33*, 1338; *Physica*, **1964**, *30*, 1109.

(54) Feynman, R. P.; Hibbs, A. R. *Quantum Mechanics and Path Integrals*; McGraw-Hill: New York, 1965.

(55) Suárez, A.; Silbey, R.; Oppenheim, I. *J. Chem. Phys.* **1992**, *97*, 5101.

(56) Pechukas, P. *Phys. Rev. Lett.* **1994**, *73*, 1060; *Phys. Rev. Lett.* **1995**, *75*, 3021. Alicki, R. *Phys. Rev. Lett.* **1995**, *75*, 3020.

(57) Oxtoby, D. W. *Adv. Chem. Phys.* **1979**, *40*, 1.

(58) Dekker, H. *Physica A* **1991**, *175*, 485.

(59) Diósi, L. *Europhys. Lett.* **1993**, *22*, 1; *Physica A* **1993**, *199*, 517.

(60) Caldeira, A. O.; Leggett, A. J. *Physica A* **1983**, *121*, 587.

(61) Hu, B. L.; Paz, J. P.; Zhang, Y. *Phys. Rev. D* **1992**, *45*, 2843.

(62) Kosloff, R.; Kosloff, D. *J. Comput. Phys.* **1986**, *63*, 363. Neuhauser, D.; Baer, M. *J. Chem. Phys.* **1989**, *90*, 4351.

(63) Landau, L. D. *Phys. Z. Sowjetunion* **1932**, *2*, 46. Zener, C. *Proc. R. Soc. London Ser. A* **1932**, *137*, 696.

(64) Frauenfelder, H.; Wolynes, P. G. *Science*, **1985**, *229*, 337.

(65) Heller, E. J. *J. Chem. Phys.* **1978**, *68*, 3891.

(66) Feshbach, H. *Ann. Phys. NY* **1958**, *5*, 357; **1962**, *19*, 287. Levine, R. D. *Quantum Mechanics of Molecular Rate Processes*; Clarendon: Oxford; 1969. Desouter-Lecomte, M.; Liévin, J.; Brems, V. *J. Chem. Phys.* **1995**, *103*, 4524. Brems, V.; Desouter-Lecomte, M.; Liévin, J. *J. Chem. Phys.* **1996**, *104*, 2222. Desouter-Lecomte, M.; Liévin, J. *J. Chem. Phys.* **1997**, *107*, 1428.

(67) Reinhardt, W. P. *Annu. Rev. Phys. Chem.* **1982**, *33*, 223.

(68) Burghardt, I.; Gaspard, P. *J. Chem. Phys.* **1994**, *100*, 6395; *Chem. Phys.* **1997**, *225*, 259.

(69) Bohm, A. *Quantum Mechanics−Foundations and Applications*; Springer: New York, 1993.

(70) Desouter-Lecomte, M.; Jacques, V. *J. Phys. B* **1995**, *28*, 3225.

(71) Gaspard, P.; Alonso, D.; Burghardt, I. *Adv. Chem. Phys.* **1995**, *XC*, 105.

(72) Feit, M. D.; Fleck, J. A.; Steiger, A. *J. Comput. Phys.* **1982**, *47*, 412.

(73) Fleck, J. A.; Morris, J. R.; Feit, M. D. *Appl. Phys.* **1976**, *10*, 129.

(74) Hellsing, B.; Metiu, H. *Chem. Phys. Lett.* **1986**, *127*, 45.

(75) Broeckhove, J.; Feyen, B.; Lathouwers, L.; Arickx, F.; Van Leuven, P. *Chem. Phys. Lett.* **1990**, *174*, 504.

(76) Jackson, B. *Chem. Phys. Lett.* **1997**, *270*, 484.

(77) Meier, C.; Tannor, D. J. In preparation.

(78) Lucke, A.; Mak, C. H.; Egger, R.; Ankerhold, J.; Grabert, H. *J. Chem. Phys.* **1997**, *107*, 8397.

(79) Reid, P. J.; Silva, C.; Barbara, P. F.; Karki, L.; Hupp, J. T. *J. Phys. Chem.* **1995**, *99*, 2609.

(80) Gardiner, C. W. *Quantum Noise*; Springer: Berlin; 1991.

(81) Lindenberg, K.; West, B. J. *The Nonequilibrium Statistical Mechanics of Open and Closed Systems;* VCH Publishers: New York, 1990.